



Cite this: *New J. Chem.*, 2020, **44**, 5638

## Naturally derived nano- and micro-drug delivery vehicles: halloysite, vaterite and nanocellulose

Anna Vikulina, <sup>\*a</sup> Denis Voronin, <sup>bc</sup> Rawil Fakhrullin, <sup>bd</sup> Vladimir Vinokurov <sup>b</sup> and Dmitry Volodkin <sup>de</sup>

Recent advances in drug delivery and controlled release had a great impact on bioscience, medicine and tissue engineering. Consequently, a variety of advanced drug delivery vehicles either have already reached the market or are approaching the phase of commercial production. Progressive growth of the drug delivery market has led to the necessity to earnestly concern about economically viable, up-scalable and sustainable technologies for a large-scale production of drug delivery carriers. We have identified three attractive natural sources of drug carriers: aluminosilicate clays, minerals of calcium carbonate, and cellulose. Three classes of drug delivery carriers derived from these natural materials are halloysite nanotubes, vaterite crystals and nanocellulose. These carriers can be produced using “green” technologies from some of the most abundant sources on the Earth and have extremely high potential to meet all criteria applied for the manufacture of modern delivery carriers. We provide an up-to-date snapshot of these drug delivery vehicles towards their use for bioapplications, in particular for drug delivery and tissue engineering. The following research topics are addressed: (i) the availability, sources and methodologies used for production of these drug delivery vehicles, (ii) the drug loading and release mechanisms of these delivery vehicles, (iii) *in vitro*, *in vivo*, and clinical studies on these vehicles, and (iv) employment of these vehicles for tissue engineering. Finally, the prospects for vehicles’ further development and industrialisation are critically assessed, highlighting most attractive future research directions such as the design of third generation active biomaterials.

Received 31st December 2019,  
 Accepted 7th March 2020

DOI: 10.1039/c9nj06470b

rsc.li/njc

<sup>a</sup> Fraunhofer Institute for Cell Therapy and Immunology, Branch Bioanalytics and Bioprocesses, Am Mühlenberg 13, 14476 Potsdam-Golm, Germany.

E-mail: [anna.vikulina@izi-bb.fraunhofer.de](mailto:anna.vikulina@izi-bb.fraunhofer.de); Tel: +49-331-58 187-122

<sup>b</sup> Gubkin Russian State University of Oil and Gas, Department of Physical Chemistry, Leninsky pr. 65-1, Moscow, 119991, Russian Federation

<sup>c</sup> Saratov State University, Educational and Research Institute of Nanostructures and Biosystems, Astrakhanskaya 83, 410012 Saratov, Russian Federation

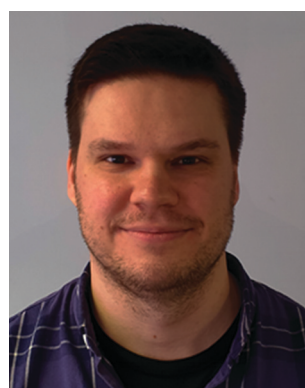
<sup>d</sup> Kazan Federal University, Institute of Fundamental Medicine and Biology, Kremly uramı 18, Kazan, Republic of Tatarstan, 420008, Russian Federation

<sup>e</sup> School of Science and Technology, Nottingham Trent University, Clifton Lane, Nottingham NG11 8NS, UK



**Anna Vikulina**

Anna Vikulina completed her PhD in the field of Biological Science in 2015. Her research interests are in the development of drug delivery carriers including naturally derived ones and the deciphering of the pathways of the biological action and transport of drugs of various natures. She has been awarded Alexander von Humboldt and Marie Curie Fellowships. Currently she is an independent research fellow in the Fraunhofer Institute for Cell Therapy and Immunology, Germany.



**Denis Voronin**

Denis Voronin completed his PhD in the field of Radiophysics in 2014. He has worked at Saratov State University, the Gubkin Russian State University of Oil and Gas (RF), and the Max-Planck Institute of Colloids and Interfaces (Germany) as a guest researcher. His major research activities lie in the field of functional nanocomposite materials and delivery systems sensitive to external physical stimuli.



## 1. Introduction

During the last few decades, emerging new drug delivery technologies allowed control of the design and fabrication of various materials at the nanoscale, which revolutionised biomedical science and significantly impacted the fields of nanomedicine, diagnostics and tissue engineering. Since drug delivery allows controlled transfer of drugs to the target with a high efficiency and minimised adverse side effects, drug delivery vehicles have progressively become an integral part of modern medications. Besides this, the costs for the development of new clinical therapeutics might be estimated as \$100–500 million, while the development of new delivery vehicles is

much less expensive and generally gives significantly quicker profit.<sup>1</sup> This provides an additional economic reason for the boost of drug delivery technologies.

Despite their promising prospects and their success in drug delivery research, new delivery vehicles are making their way from science to the market extremely slow. This is due to multiple factors, and most of them are not related to science and range from rather complicated policies and procedures for Food and Drug Administration (FDA) agency approval to high fabrication costs that largely pose a manufacturing challenge. Indeed, sometimes the costs for manufacturing drug delivery vehicles much exceed the costs for the drug itself. For instance, liposomal doxorubicin Doxil (the drug widely used for the treatment of ovarian cancer, sarcoma and myeloma) costs *ca.* \$130 per unit, which is 40–100 times higher than that of free doxorubicin (*ca.* \$1.3–3 per unit; USA prices). Another complication is a multi-step fabrication of drug delivery carriers that is often challengeable to upscale, at least using modern technologies. For instance, upscaling remains a serious limitation for the commercialisation of polymeric nanoparticles.<sup>2</sup> Finally, the use of animal and plant sources for the isolation of substances for delivery carriers (*e.g.* lipids, biopolymers, proteins) is quite common.<sup>3</sup> Low sustainability of delivery carriers production stimulates scientists to think about the possible negative environmental impact that the global production of delivery vehicles may have.<sup>4</sup>

In view of the above, the quest for alternatives sources for drug delivery vehicles – minerals, bacteria and waste materials – resulted in the rise of a new wave of drug delivery research. Scientists have proposed dozens of novel drug delivery vehicles, the most important examples of which are clays, minerals of calcium salts such as carbonates and hydroxyapatites, and cellulose-based materials. Typical examples of nano- and micro-sized particles made of such materials are halloysite nanotubes (HNTs), vaterite CaCO<sub>3</sub> (VCC) and nanocellulose (NC).



**Rawil Fakhrullin**

*Rawil Fakhrullin is a Professor at the Institute of Fundamental Medicine and Biology, Kazan Federal University (Republic of Tatarstan, RF). He received his PhD in 2006 from KFU. He has worked as a visiting scientist in the Universities of Hull and Sheffield (UK), Yeditepe University (Turkey), and Louisiana Tech University (USA). He has published >100 peer-reviewed papers and edited 4 books. In 2016, he was conferred the title of visiting professor by the University of Palermo (Sicily, Italy), in 2017 he was admitted as a Fellow to the Royal Society of Chemistry. His research interests are focused on the development of novel biomimetic materials, cell-based therapy, and drug delivery using nanoclays as natural sources.*

*Rawil Fakhrullin is a Professor at the Institute of Fundamental Medicine and Biology, Kazan Federal University (Republic of Tatarstan, RF). He received his PhD in 2006 from KFU. He has worked as a visiting scientist in the Universities of Hull and Sheffield (UK), Yeditepe University (Turkey), and Louisiana Tech University (USA). He has published >100 peer-reviewed papers and edited 4 books. In 2016, he was conferred the title of visiting professor by the University of Palermo (Sicily, Italy), in 2017 he was admitted as a Fellow to the Royal Society of Chemistry. His research interests are focused on the development of novel biomimetic materials, cell-based therapy, and drug delivery using nanoclays as natural sources.*



**Vladimir Vinokurov**

*Vladimir Vinokurov is Professor and Chair of Physical and Colloid Chemistry at the Gubkin Russian State University of Oil and Gas. He pioneered a number of colloidal formulations for diverse applications protected with 27 Russian patents and published >200 peer-reviewed papers on organic-inorganic nano- and micro-composites. His recent research activities include micro- and nanocellulose-based hybrid materials for biomedical applications.*



**Dmitry Volodkin**

*Dmitry Volodkin is Associate Professor at Nottingham Trent University. He studied Chemistry at Lomonosov Moscow State University; further research stays brought him to France (University of Strasbourg) and Germany (Max-Planck Institute of Colloids and Interfaces, TU Berlin, Fraunhofer IZI-BB). His research activities are focused on advanced stimuli-responsive biomaterials for applications in tissue engineering, diagnostics, toxicology, and drug delivery. His group engineers hybrid structures with a main focus on the utilization of biocompatible mesoporous vaterite crystals. D. V. has published >80 peer-reviewed papers and received the prestigious Sofja Kovalevskaja Award and Richard-Zsigmondy Prize, and Alexander von Humboldt and Marie Curie Fellowships.*



**Table 1** Estimated material costs for the production of different drug delivery vehicles<sup>a</sup>

Drug delivery vehicles	Price, \$ per g of dried weight
Liposomes (DPPC)	90–170
PLGA (50:50, 1–2 dL g <sup>-1</sup> )	30–70
Halloysite nanotubes	0.3–0.4
Vaterite CaCO <sub>3</sub>	0.2–0.4 <sup>b</sup>
Nanocellulose	0.8–5.5

DPPC – dipalmitoylphosphatidylcholine; PLGA – poly(lactic-co-glycolic acid). <sup>a</sup> Lab grade chemicals; prices provided by official distributors – Sigma Aldrich; Merck; Fisher Scientific; Polysciences; Cellulose Lab; Avanti Polar Lipids, *etc.* <sup>b</sup> Produced from CaCl<sub>2</sub>·2H<sub>2</sub>O and Na<sub>2</sub>CO<sub>3</sub>.

All these materials exhibit null to low toxicity, good biocompatibility and/or biodegradability. These delivery vehicles may be loaded with tremendously diverse compounds ranging from small drugs to macromolecules and from highly hydrophilic to solely lipophilic encapsulates. Importantly, material costs required for their production are significantly lower than those for conventional delivery vehicles (Table 1). A variety of fabrication technologies proposed during the last few decades lays a platform for their swift industrialisation.

In addition to lower material costs, production of HNTs and NC is commonly reduced to their isolation and purification from abundant sources (Fig. 1), which is generally less expensive compared to sophisticated methods for the fabrication of conventional vehicles such as liposomes and polymer beads. Calcium carbonate is also an abundant natural mineral that can be isolated from natural sources; however, the most common in nature is calcite, a nonporous polymorph of CaCO<sub>3</sub>, while mesoporous VCC (more suitable for biomedical applications) is not so abundant. Because of low abundance of vaterite in nature, its bottom-up production is economically more profitable. NC growth by bacteria is also widely proposed as a sustainable alternative to plant-derived sources. Moreover, “green” strategies for the production of nanocellulose from wood or paper waste<sup>5,6</sup> as well as vaterite from eggshell and seashell waste<sup>7,8</sup> are now being widely discussed.

Although these “sustainable” delivery vehicles have not dislodged their conventional analogies yet, they have rapidly gained popularity and have extremely high potential to enter the market of drug delivery vehicles in the nearest future.

In this paper, we discuss the up-to-date knowledge on and prospects for biomedical use of three naturally derived delivery vehicles: HNTs, VCC, and NC. All of them have been known for

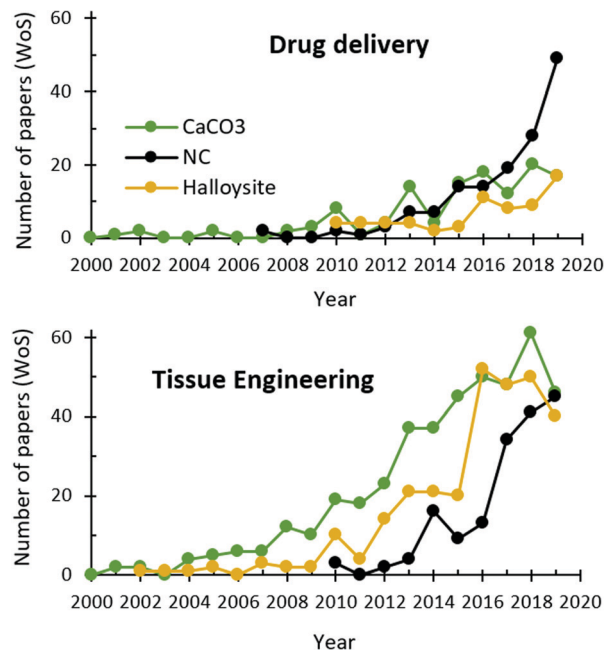


**Fig. 2** Annual numbers of scientific research publications on the topics “halloysite”, “calcium carbonate” and “nanocellulose” and “drug delivery” or “tissue engineering” in the past two decades (Web of Science Database, November 2019).

ages but discovered as drug delivery vehicles quite recently and witnessed an exponential growth of scientific interest since that time (Fig. 2). This article aims at uncovering key features of HNTs, VCC and NC in a comparative manner, revealing their strong and weak sides for drug delivery and tissue engineering/regeneration applications, and evaluating the prospects for their further study and biomedical use.

## 2. Clay nanotubes

### 2.1. Clay-based nanomaterials

Among the variety of different minerals, clay minerals are the most widely used for therapeutic purposes due to their high specific area, chemical and mechanical stability, biocompatibility and low toxicity for humans. Nanoclays are largely abundant in nature, which eliminates the need for their industrial synthesis. The only exception is LAPONITE<sup>®</sup>, a synthetic equivalent of

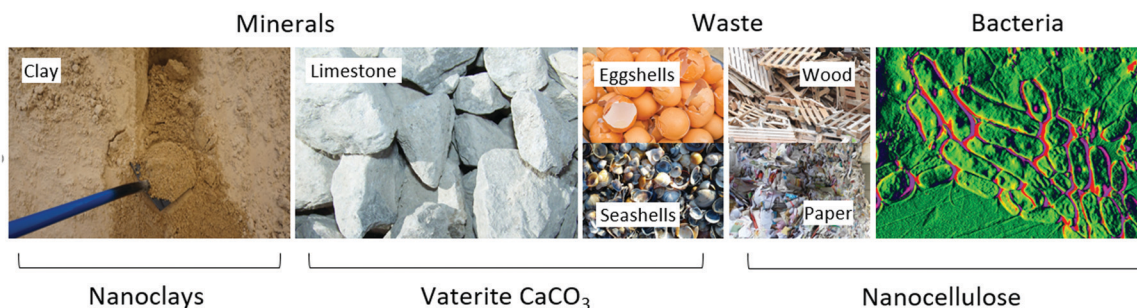


**Fig. 1** Sustainable sources of nanoclays, calcium carbonate and nanocellulose.



hectorite produced by Laporte (Netherlands). Other nanoclays exist in nature; these minerals refer to the group of phyllosilicates, also called “sheet silicates”. Nanoclays are hydrous alumina or magnesium silicates (sometimes with variable amounts of other metals) composed of parallel sheets of Si–O tetrahedral and octahedral sheets containing metal atoms (Al, Mg) coordinated with the oxygen from Si–O tetrahedra and OH groups.

Nanoclays are very diverse and classified based on the number of tetrahedral and octahedral sheets per clay layer as 1:1, 2:1 and 2:1:1 minerals. Thus, kaolinite and halloysite (Fig. 3), the polymorphs of  $\text{Al}_2\text{Si}_2\text{O}_5(\text{OH})_4$ , are 1:1 clays in which one octahedral sheet is bonded to one tetrahedral sheet, yielding a 7 Å repeat along the z-axis. These layers may have lateral dimensions from tens of nanometres to micrometres.<sup>9</sup> Several layers may interact with each other *via* electrostatics and van der Waals interactions, hydrogen bonding or interlayer cations that ensure the diversity of nanoclays. The mineralogical properties of nanoclays are described in detail in a recent review.<sup>10</sup>

Halloysite is a significant component of many kaolinitic clays that commonly exists in a mixture with kaolinite, silica, or other mineral contaminants. Production of pure HNTs requires careful separation of halloysite from accompanying minerals and therefore the economical costs of HNTs directly depend on the initial purity of halloysite deposits. In this respect, two main sources of HNTs are located in Northland, New Zealand, and Utah, USA, where large deposits of high-grade halloysite are found. Smaller or lower-grade deposits are also found in many countries in Asia, South America, Australia,

and Europe.<sup>13</sup> Annually, about 30 kilotonnes of halloysites are excavated and processed into dispersed nanotubes.<sup>14</sup>

Although no direct approval of HNTs has been done by the FDA so far, kaolin (a mineralogical group of clays to which halloysite also belongs) is approved as an indirect food substance generally recognised as safe (*e.g.* as a possible component of paper and paperboard that contact food) under §186.1256. Besides this, colloidal kaolin is approved as a “drug product containing certain active ingredients offered over-the-counter”, §310.545, with the note that there are inadequate data to properly assess its safety and effectiveness. Therein, kaolin is proposed as an antidiarrheal drug product.

The fact that clays are generally recognised as safe for humans makes biomedical use of nanoclays and in particular HNTs highly promising. The next two sections describe advantages, limitations and up-to-date achievements in utilisation of HNTs in drug delivery and tissue engineering.

## 2.2. HNTs for drug delivery

### 2.2.1. Drug loading and release.

Loading of the molecules of interest into HNTs is determined by Si–OH and Al–OH functional groups existing on their external and internal surfaces, respectively. Deprotonation of silanol groups is responsible for the negative net charge of HNTs at pH above 3. Consequently, the anionic nature of the external HNT surface enables it to interact with cationic compounds, while aluminol groups located on the internal lumen surface carry positive charge and support the loading of anionic molecules. In addition to electrostatics, interaction of molecules and their assemblies with HNTs might involve hydrogen binding, van der Waals and other specific interactions.<sup>15</sup>

In general, bare HNTs exhibit weak bonding with drugs. Chemical modification of both the inner lumen and the outer surface is a general strategy to tune the capacity and drug delivery performance of HNTs.<sup>16</sup> Multiple Si–OH and Al–OH groups present at the HNT surface provide various ways for this modification. The lumen covered with Al–OH groups can be grafted with organosilane and organophosphonic acid.<sup>17</sup> For instance, the functionalisation of HNTs with (3-aminopropyl)triethoxysilane (APTES) introduces hydrogen-binding sites and thus enhances the retention of drugs that are prone to form H-bonds.<sup>18</sup> Insights into the surface modification of HNTs are substantially described in reviews 15 and 19. The external surfaces of HNTs can be coated with positively charged polymers. Thus, grafting of HNTs with an amine of polyethylene glycol enhanced cellular uptake and improved the loading of low water-soluble antioxidant quercetin.<sup>20</sup>

Undoubtedly, the possibility of both loading a drug into the lumen and grafting it to the outer surface offers some advantages for drug delivery. HNTs are suitable for entrapment of various drugs (analgesics,<sup>18,21</sup> anticancer drugs,<sup>22,23</sup> antibacterials,<sup>24</sup> *etc.*) and especially attractive for the entrapment of large macromolecules (genes,<sup>25</sup> enzymes<sup>26</sup>) and nanoparticles (quantum dots,<sup>27</sup> metal nanoparticles,<sup>28</sup> more examples reviewed in ref. 29), whose sizes correlate well with the diameter of the lumen. Some recent reviews have described the loading of molecules and particles of various natures in more detail.<sup>24,30,31</sup>

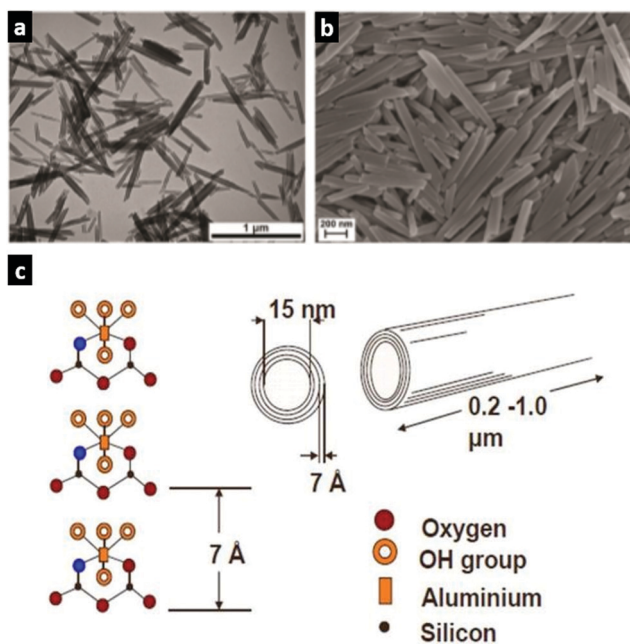


Fig. 3 Morphology and crystal structure of halloysite nanotubes: (a) TEM image and (b) SEM image of HNTs. Adopted with the permission from ref. 11, copyright© 2019 John Wiley & Sons. (c) Crystal structure and dimensions of HNTs. Adopted with the permission from ref. 12, copyright© 2008, American Chemical Society.



Some recent studies have indicated that HNTs are excellent tablet excipients (e.g. if mixed with passive components such as microcrystalline cellulose<sup>32</sup> and starch<sup>33</sup> or layered with alginate and chitosan<sup>34</sup>) due to their powder flow and compressibility properties.

Owing to the fact that HNTs have different sites for drug loading, it is not surprising that the release of the payload directly depends on the way in which the drug was loaded. Thus, the release of drugs from the lumen is mostly controlled by the diffusion of the drug molecule from the nanotube interior that is substantially retarded by the 1D nanotube structure. Thus, the release of analgesics (ibuprofen,<sup>18</sup> aspirin,<sup>35</sup> sodium salicylate<sup>36</sup>) from bare HNTs obeys the Fickian diffusion model. Different modifications of the HNT lumen allow adjusting the affinity of the drug to the HNTs and therefore controlling the release rate.<sup>18,36</sup> For instance, the release of ibuprofen from APTES-modified HNTs is governed by non-Fickian diffusion due to the additional electrostatic binding of the drug to the APTES-coated lumen that ensures slower release compared to unmodified nanotubes.<sup>18</sup> Besides this, the functionalization of HNTs with stimuli-responsive materials (e.g. pH-responsive polymers,<sup>22</sup> thermosensitive polymers,<sup>37</sup> magnetic nanoparticles<sup>38</sup>) allows tuning the release profile over a much wider range, e.g. for achieving sustained release for days<sup>38</sup> and sometimes weeks.<sup>22</sup> Alternatively, clogging of the ends of the tubes with polymers (e.g. dextrin<sup>39</sup>) allows controlling the release and extending it up to weeks. This strategy and other strategies are reviewed in ref. 40. The release of drugs linked to the external surfaces of HNTs strongly depends on the nature of drug-surface binding. Since this binding often involves strong covalent interactions,<sup>41</sup> the release of drugs from the outer surface might be slow, prolonged and sometimes incomplete as was demonstrated for curcumin covalently linked to the outer surfaces of the HNTs.<sup>41</sup>

### 2.2.2. Cellular uptake, cytotoxicity and *in vivo* studies.

Some recent studies have indicated that HNTs internalize into cells *via* endocytosis. After entering the cells, HNTs are predominantly transported into Golgi apparatus and lysosomes by microtubules and actin filaments.<sup>42</sup> Later, an *in vitro* study of HNTs functionalised with hydrophobic coatings showed their binding to the cell membrane and decrease in their lysosomal activity.<sup>43</sup> These studies open avenues for site-specific intracellular delivery using HNTs.

Numerous *in vitro* studies have pointed out no or a rather low toxicity of HNTs.<sup>44,45</sup> This was also confirmed in *in vivo* studies on nematodes<sup>46</sup> and zebrafish.<sup>47</sup> The effect of HNTs on cells is dose-dependent as has been shown for human cell lines.<sup>48</sup> Recently, the size-dependent character of cellular internalisation of HNTs (250–650 nm in length) has been demonstrated in colon cancer cells.<sup>49</sup> A toxic effect was reported only when high doses of HNTs were orally administered into mice, while low and moderate doses remain non-toxic.<sup>50</sup> Since HNTs are non-toxic even at high doses (concentrations of 1000  $\mu\text{g mL}^{-1}$  and higher<sup>46</sup>), they can be suitable for nearly all administration routes. For instance, HNTs loaded with a neurotransmitter ( $\gamma$ -aminobutyric acid) were successfully attempted for delivery to the brain.<sup>51</sup> Functionalisation of HNTs with mucoadhesive polymers enhances their interactions with intestinal cells and causes no cytotoxicity.<sup>52</sup>

Topical administration of HNT coatings on hair surfaces was recently proposed. Inclusion of selected dyes or drugs into HNTs prior to their application allows for hair coloring or medical treatment, respectively.<sup>53</sup>

Recent *in vivo* studies confirmed the potential of HNTs as effective drug delivery containers, showing that treatment with curcumin-loaded HNTs suppresses the growth of pathogenic bacteria in *C. elegans* and completely restores the longevity of infected nematodes.<sup>54</sup> An *in vivo* study of pharmacokinetics revealed that an orally administered suspension of fluorescently labelled HNTs is not absorbed by the intestines and eliminated *via* feces within one day, while systemically administered nanotubes are eliminated *via* urine/feces within nearly 72 h.<sup>55</sup> Notably, although in this study and some other studies<sup>23</sup> HNTs are intravenously injected, HNTs are non-biodegradable in blood. Indeed, recent studies have not recommended direct injections of HNTs that may lead to a thrombosis.<sup>45</sup> Besides this, a recent study demonstrated that inhalation of HNTs may cause oxidative stress, inflammatory response, and autophagy and therefore results in sub-chronic toxicity in mice.<sup>56</sup> However, this does not hinder the use of HNTs for drug delivery *via* alternative routes as well as their use in tissue engineering.

### 2.3. HNTs for tissue engineering

In recent years, functionalisation of natural and synthetic polymer scaffolds with nanoscale dopants has been widely attempted. Among others, HNTs have shown great promise as an additive to polymeric tissue engineering scaffolds due to their excellent biocompatibility and controlled drug delivery behaviour. Importantly, HNTs can be mixed with almost any materials used for scaffold fabrication employing traditional polymer blending methods. It has been verified that the introduction of only a few wt% of HNTs leads to a significant improvement of scaffold materials. At the same time, the incorporation of extremely high contents of HNTs (up to 80 wt%) can be safely used to form hard tissue substitutes.<sup>57</sup>

With respect to tissue engineering applications, the use of HNTs promotes the attachment, viability, proliferation, adhesion, and growth of cells and improves the mechanical and thermal stability of scaffolds, having no negative impact on the biocompatibility of the scaffolds.<sup>58,59</sup> The good blood compatibility of HNT-doped scaffolds has also been confirmed by haemolysis tests.<sup>59</sup> Later, blood vessel formation around HNT-doped polymer 3D scaffolds has been demonstrated.<sup>60</sup> The scaffolds used in this study are shown in Fig. 4.

Besides this, HNT-doped scaffolds benefit from the loading of the nanotubes with various functional compounds such as antimicrobial agents<sup>61,62</sup> and the cues essential for tissue regeneration (e.g. growth factors<sup>63</sup>).

Most of these studies have focused on *in vitro* evaluation using model cell lines and stem cells. *In vivo* case studies are still rather limited. Examples include (i) functionalised wound dressing materials like HTNs/chitosan<sup>64</sup> and HNTs/poly(L-lactide)<sup>61</sup> which demonstrated improved skin reepithelialization; (ii) nanocomposites for bone tissue regeneration<sup>65</sup> wherein HNTs themselves stimulated osteogenic differentiation of cells and improved



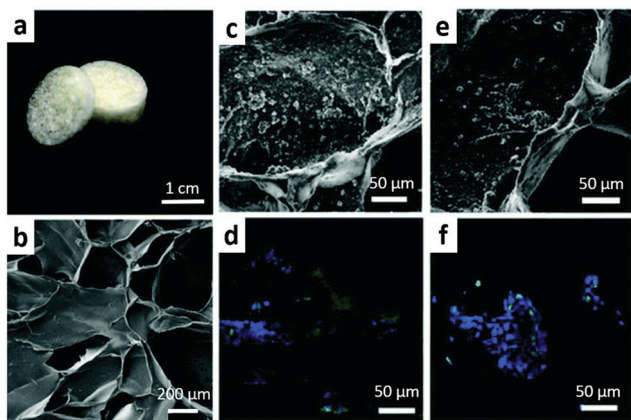


Fig. 4 (a) Photograph and (b) SEM image of pillar-shaped 3D porous hydrogel scaffolds functionalised with 6 wt% of HNTs and SEM and confocal images of (c and d) A549 and (e and f) Hep3B cell distributions on them. Adopted with permission from ref. 60, copyright© 2016, Royal Society of Chemistry.

bone repair; (iii) HNT-functionalised alloys with improved corrosion resistance for orthopaedic applications<sup>66</sup> and (iv) aligned composites with HNTs for guided nerve regeneration.<sup>63</sup>

### 3. Calcium carbonate

#### 3.1. CaCO<sub>3</sub> and its polymorphs

Anhydrous calcium carbonates exist in the form of one of the three main polymorphs: calcite, aragonite, or vaterite. All the polymorphs may be found in nature.<sup>67</sup> Calcite is the major component of carbonate rocks and hard tissues in marine organisms (seashells) and eggshells. Although traces of vaterite and slightly more abundant amounts of aragonite were found in mollusc pearls, fish otoliths, and ascidians,<sup>67</sup> calcite represents the only stable phase of anhydrous CaCO<sub>3</sub> and thus much dominates over less stable vaterite and aragonite. Unfortunately, the most common calcite is of least interest for biomedical applications due to its non-porous structure and thus low capacity for drug loading. As opposed to calcite, crystals of aragonite and especially vaterite have a highly developed internal structure suitable for hosting molecules of interest of various natures; this largely determined the use of vaterite in nanomedicine.

Unfortunately, the occurrence of vaterite in nature is low. Vaterite can be (bio)mineralised by some calcifying bacteria, yet this approach is rather expensive.<sup>68</sup> Therefore, the main source of vaterite remains calcite. Direct transformation of calcite to vaterite or aragonite is thermodynamically restricted,<sup>69</sup> nevertheless, vaterite can be synthesized from calcite in a few steps. First, CaCO<sub>3</sub> in the form of calcite is degraded by the so-called Solvay process in a reaction with NaCl to produce its soluble salts (e.g. Na<sub>2</sub>CO<sub>3</sub> and CaCl<sub>2</sub>). In much of the world, this is the major industrial process for the production of sodium carbonate, wherein CaCl<sub>2</sub> is the by-product. Second, CaCO<sub>3</sub> in the form of vaterite can be precipitated from Na<sub>2</sub>CO<sub>3</sub> and CaCl<sub>2</sub> upon mixing solutions of these precursor salts.<sup>70</sup> Nowadays, limestone is the primary source of calcite used for the Solvay process.

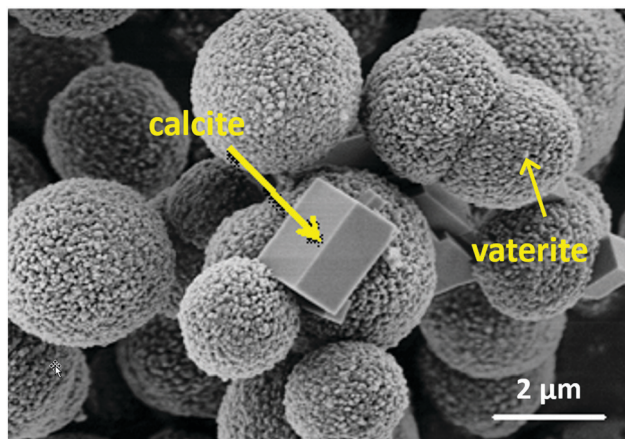


Fig. 5 SEM image of CaCO<sub>3</sub> crystals demonstrating the mesoporous nature of spherical vaterite and non-porous calcite crystals. Adopted from ref. 77, copyright© 2019, Elsevier.

Nevertheless, the use of waste materials – seashells<sup>7</sup> and eggshells<sup>8</sup> – is an excellent green alternative to rocks, which makes industrially produced vaterite an even more attractive material in future applications.

In view of high interest in VCC, its structure was widely investigated.<sup>69,71</sup> VCC comprises of small nanocrystallites aggregated together (Fig. 5). The spaces between these nanocrystalline form interconnected cylindrical pores that are usually in the range of a few tens of nm. Therefore, VCC belongs to mesoporous materials. VCC crystals have typical dimensions ranging from 3 to 20 μm and most often have a spherical shape. A number of recent studies have also proposed novel ways for the fabrication of VCC nanocrystals<sup>72–74</sup> indispensable for drug delivery applications. The shape and morphology of these crystals may be tuned over a wide range using organic solvents<sup>73</sup> or mild water–urea mixed systems,<sup>75</sup> polymer matrices and proteins<sup>74</sup> or nanoparticles.<sup>76</sup> The porosity of the crystals can be controlled *via* the variation of preparation temperature with no additives.<sup>70</sup>

The FDA has approved the use of CaCO<sub>3</sub> (without specifying its polymorphism) as a food additive (§582.1191), a dietary supplement (§582.5191), a direct food substance (§184.1191), and a colour additive for food (§73.70) and drugs (§73.1070). Similar to kaolin clay, calcium carbonate is also mentioned in §310.545, where it is proposed as an antidiarrheal, digestive and weight control drug product. CaCO<sub>3</sub> is registered as a food additive (white food colouring) under E170 code. As a dietary supplement, calcium carbonate may be prescribed when calcium taken in the diet is deficient. It comes in the form of tablets, capsules, or suspensions taken orally and sold under such brands as Calel-D<sup>®</sup>, Calcid<sup>®</sup>, and Os-Cal 500<sup>®</sup>. The wide use of CaCO<sub>3</sub> in food preparation and the diet premises safe-by-design utilisation of CaCO<sub>3</sub> as a drug vehicle in future applications.

#### 3.2. VCC for drug delivery

**3.2.1. Drug loading and release.** The mesoporous structure of VCC serves as a host for various encapsulates ranging from small molecules (anticancer drugs,<sup>78</sup> anaesthetics,<sup>79</sup> antibiotics<sup>80</sup>)



to macromolecules (proteins,<sup>77,81,82</sup> growth factors,<sup>83</sup> genes<sup>84,85</sup>) and inorganic nanoparticles (Ag,<sup>86</sup> TiO<sub>2</sub>,<sup>87</sup> Fe<sub>3</sub>O<sub>4</sub><sup>76,88</sup>). Importantly, multicomponent encapsulation into VCC is also possible and has been reported (*e.g.* doxorubicin and tumour-suppressing microRNA<sup>84</sup>).

Typical pores of VCC are in the range of a few tens of nm that in general makes the encapsulation of large molecules/particles more effective when compared to small drugs. In order to overcome the relatively low capacity of crystals to small molecules, the internal volume of the crystals can be filled with a polymer matrix that has high affinity to desired drugs. This strategy to make composite hard-soft vehicles has been widely reported. Examples include cyclodextrin-CaCO<sub>3</sub> hybrids designed as carriers for hydrophobic drugs and hormones.<sup>89</sup> Carrageenan-CaCO<sub>3</sub><sup>90</sup> and mucin-CaCO<sub>3</sub> hybrids<sup>91</sup> were produced to host doxorubicin, *etc.* Besides enhancing loading capacity for small drugs, the inclusion of polymers inside crystals may also stabilise them and slow down the VCC recrystallization to calcite that is important for modulating the drug release profile.<sup>91</sup>

Loading of molecules into VCC can be performed under mild conditions either during crystal growth (this approach is usually denoted as co-precipitation or co-synthesis<sup>76,92</sup>) or by means of post-loading into pre-formed VCC crystals (*e.g. via* adsorption into crystal pores<sup>92</sup> or a recently introduced freeze-drying approach<sup>93</sup>). Among these approaches, adsorption and co-synthesis are two primary methods for drug encapsulation. Adsorption represents the most “mild” method suitable for the encapsulation of labile molecules prone to aggregation, denaturation and the loss of activity in aggressive media.<sup>81,82,94</sup> In contrast, for co-precipitation mixing of drug solution with precursor salts results in more effective entrapment and homogeneous distribution of the drug inside the crystals during their growth. However, because of more harsh conditions of crystal growth (high ionic strength and elevated pH), much higher encapsulation efficiencies may be accompanied by a partial loss of activity for sensitive macromolecules,<sup>81</sup> while small drugs are usually unaffected. Finally, crystals loaded by means of adsorption are usually prone to faster drug release than crystals loaded by co-synthesis.<sup>82</sup>

Crystal coating with lipids,<sup>95</sup> polymers<sup>79</sup> or polymer multilayers<sup>76</sup> fabricated *via* polymer layer-by-layer assembly is often proposed to reduce drug leakage and prolong drug release kinetics. Notably, polymer multilayers are permeable for ions and small molecules, which allows the formation of polymer based capsules when multilayer coated VCC crystals are decomposed by lowering the pH or adding chelating agents (*e.g.* ethylenediaminetetraacetic or citric acid). CaCO<sub>3</sub>-templated multilayer capsules are very promising delivery vehicles; their potential for drug delivery has been widely investigated,<sup>96–99</sup> this also includes *in vitro*<sup>97</sup> and *in vivo* studies.<sup>98</sup> This article does not consider VCC-templated capsules and beads;<sup>100</sup> for these topics the reader can refer to reviews 101 and 102.

The release of drugs from VCC is governed either by VCC dissolution or by VCC recrystallization. Thus, dissolution-mediated release occurs in case of intracellular VCC delivery, when VCC entrapped inside lysosomes is influenced by acidic lysosomal pH (~4.5–5.0) that promotes VCC dissolution and

results in release of the loaded molecules.<sup>78</sup> Recent studies of the use of VCC as an anticancer drug delivery vehicle have shown an interesting possibility for employing VCC sensitivity to acidic pH to target the release selectively on a tumor microenvironment that has pH slightly below 7.<sup>95,103,104</sup> Later, this approach has shown to be effective not only for *in vitro* but also for *in vivo* studies. It is worth noting that targeting an acidic tumor microenvironment is quite a versatile approach for anticancer therapy and has been successfully employed not only for VCC but also for other carriers, *e.g.* polymeric nanoparticles;<sup>105</sup> this supports the potency of this strategy. The pH sensitivity of VCC crystals limits their oral administration (at least if the crystals are not functionalized) due to the swift VCC dissolution and the loss of the payload in the stomach (pH ~ 1.5–3.5).

Recrystallization-mediated release occurs due to the phase transition of thermodynamically unstable vaterite to more favorable and non-porous calcite with much lower surface area and therefore much lower drug capacity.<sup>77,91,106</sup> Recrystallization and, as a result, release kinetics can be effectively controlled *via* the use of additives that fill the pores of the crystals. For instance, hybrids of VCC with ferromagnetic nanoparticles recrystallize to calcite significantly more rapidly than bare vaterite crystals, while multilayer coating or the co-precipitation of the polymers into VCC crystals may decelerate vaterite → calcite transformation.<sup>76,91</sup> Notably, plasma proteins like bovine serum albumin (BSA) may also significantly adsorb to the surfaces of VCC crystals, which is of high importance for intravenous administration. Plasma proteins not only suppress the VCC recrystallization and therefore allow prolonged circulation of the crystals but also minimize the neutrophil activation caused by VCC binding to the membranes of the neutrophils.<sup>107</sup>

**3.2.2. Cellular uptake, cytotoxicity and *in vivo* studies.** Up to now, there have been a limited number of *in vitro* and also *in vivo* studies of employment of VCC crystals as drug delivery vehicles. All *in vitro* trials show no cytotoxicity and no influence on cell viability,<sup>108</sup> even at enormously high concentrations.<sup>109</sup> Intracellular VCC uptake does not cause any elevation of caspase or Bcl-2/Bax activity, which indicates no initiation of apoptosis.<sup>110</sup> The rate of the penetration of drug-loaded vehicles and cellular response depend on the size and the shape of VCC.<sup>111</sup> Although oral delivery of VCC is limited by its high solubility in acidic media, recent studies proposed various alternative routes of administration.

Thus, intravenous injections were applied for the treatment of cancer in mouse models wherein VCC crystals were used as carriers either for doxorubicin employed in chemotherapy<sup>95,104</sup> or for cocktails of catalase, fluorescent probes with two-photon excitation, and traditional photosensitizers, *i.e.* as a platform for photodynamic therapy.<sup>112</sup> Both studies have revealed high promise of the use of VCC crystals. In general, anticancer drug delivery seems to be a major biomedical application of VCC attempted so far. Along with the targeting the acidic tumor microenvironment mentioned above, there are some other advantages of VCC. One of them is simple one-step loading of VCC with multiple functional components, *e.g.* combinations of magnetic nanoparticles and anticancer drugs, which allows



external navigation of VCC to tumor sites.<sup>113</sup> Similarly, VCC crystals loaded with glucose oxidase and  $\text{Fe}_3\text{O}_4$  have been proposed for chemodynamic therapy *via* the ultrasound-assisted Fenton reaction.<sup>114</sup>

In view of the high promise of VCC employment in mucosal drug delivery,<sup>99,115</sup> a recent report demonstrated an *in vivo* study of intranasal delivery into the brain using VCC pre-loaded with an anesthetic drug.<sup>79</sup> Interestingly, VCC crystals of different sizes ranging from nano- to micro-dimensions have been probed in this study, demonstrating that the micron-sized crystals ensure a more prolonged anesthetic effect than the nano-sized ones, while both are suitable carriers for intranasal delivery. Besides this, transdermal,<sup>116</sup> ocular<sup>77</sup> and pulmonary delivery<sup>117</sup> of VCC crystals have been attempted.

Although the studies described above revealed the high potential of VCC for drug delivery and laid a platform for further clinical studies, VCC-based delivery requires much more investigations and solid basic research prior to translation into practical use. Key milestones of further VCC development as delivery vehicles are highlighted in the last section of this article.

### 3.3. VCC for tissue engineering

Nowadays, VCC crystals are primarily used for bone tissue engineering and repair which is not surprising considering that  $\text{CaCO}_3$  is a natural Ca-containing compound and may be used as a mineral storage material or a source of  $\text{Ca}^{2+}$  for transformation to hydroxyapatite in bone regeneration.<sup>120</sup> VCC has an excellent osteoinductivity, highly developed surface area suitable for tissue growth, suitable mechanical properties and

specific binding sites for BMP-2.<sup>121</sup> VCC plays a dual role – being a reinforcement component that provides proper mechanical support and a mineral source of  $\text{Ca}^{2+}$  essential for bone repair. In addition, VCC may be preloaded with biofactors essential for tissue growth and regeneration for sustained release. This has been shown for both small drugs (*e.g.* tannic acid releasing for weeks<sup>122</sup>) and biomacromolecule RNase.<sup>123</sup>

Most of the  $\text{CaCO}_3$ -based scaffolds are composites made of polymer hydrogels with VCC crystals embedded into polymer networks and either homogeneously distributed inside gels<sup>123,124</sup> or representing coatings, *e.g.* on polymeric polycaprolactone fibers (Fig. 6a and b).<sup>118,122</sup>

Scaffolds based on siloxane-containing VCC and biodegradable polymers occupy a separate niche.<sup>83,125</sup> VCC doped with siloxane is used as a source for soluble silica that stimulates the proliferation/differentiation of bone-forming cells and may be released for months.<sup>83</sup> In view of the topic of this article, it seems interesting to highlight the study on the design of hybrid bacterial cellulose and  $\text{CaCO}_3$  (that was in the form of a vaterite–calcite mixture).<sup>126</sup> The authors of this study highlighted the biodegradability and environmentally friendly fabrication of such scaffolds. In another study,<sup>127</sup> scaffolds containing siloxane–poly(lactic acid)–VCC hybrids with hydrated aluminum silicate nanotubes (imogolite) allowed improving the hydrophilicity and enhancing the cellular compatibility of the scaffolds, which is an important issue at the early stage after implantation.

There are multiple examples of *in vitro* verification of the osteogenic potential of VCC-based scaffolds. The *in vivo* performance of 1  $\mu\text{m}$  sized VCC crystals functionalised with heparin,

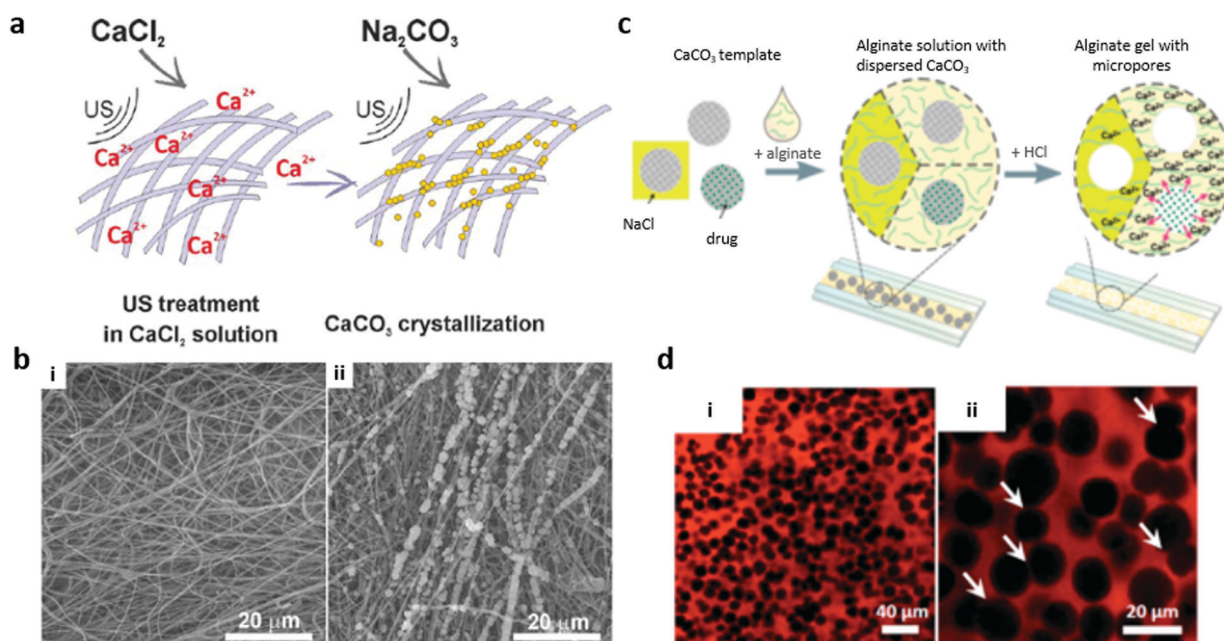


**Fig. 6** 3D polymer scaffolds fabricated using VCC as a coating (a and b) or a sacrificial porogen (c and d). (a) The scheme of fibrous material mineralization under ultrasound treatment and (b) the corresponding SEM images of blank poly( $\epsilon$ -caprolactone) fibrous material (i) and poly( $\epsilon$ -caprolactone) material mineralized with VCC (ii). Adopted from ref. 118, copyright© 2017 John Wiley & Sons. (c) The scheme of microfluidics-assisted porous alginate hydrogel fabrication and (d) CSLM images of final porous alginate scaffolds (red) formed by compact packing of VCC crystals of different sizes (i and ii) using 5% alginate and HCl. White arrows indicate some interconnected pores. Adopted from ref. 119, copyright© 2015 John Wiley & Sons.





loaded with BMP-2, and entrapped into a fibrin based hydrogel was evaluated in repair of rabbit tibia bone. Bone defects almost completely healed after 8 weeks.<sup>121</sup> Electrospun scaffolds mineralised with VCC crystals were implanted into rats, showing enhanced cell colonization and tissue vascularization as well as sustained release of tannic acid.<sup>122</sup>

VCC can serve as a sacrificial template for formulation of polymer-based scaffolds with tailor-made properties such as well-defined internal structures and compositions. Macroporous Ca-alginate scaffolds<sup>119,128</sup> (Fig. 6c and d) and those made of interconnected polymer multilayer shells<sup>129</sup> have been reported. VCC plays roles of a crosslinker and a porogen agent, allowing the filling of pores with active molecules. Such scaffolds are very soft (a few kPa), which opens new avenues to employ VCC for soft tissue engineering.<sup>130</sup>

## 4. Cellulose

### 4.1. Cellulose-based materials

Cellulose is a natural polysaccharide that is referred to as the most abundant biopolymer on Earth. The cellulose molecule consists of  $\beta$ -D-glucopyranose rings forming monomeric units (Fig. 7a), which in turn are organized in a cellulose network due to intra- and inter-molecular hydrogen bonding. Cellulose molecules possess both hydrophobic and hydrophilic parts, making them insoluble in water.<sup>131</sup> The molecular structure gives rise to some beneficial properties of cellulose like biocompatibility, biodegradability, mechanical strength and a number of hydroxyl groups suitable for surface modification.<sup>132</sup> Additionally, cellulose is a semicrystalline polymer consisting of crystalline and amorphous parts that are characterized by strong and weak hydrogen bonding, respectively. This opens an avenue for the preparation of various cellulose nano-sized carriers from cellulose nanofibers by multiple processing approaches.

Natural cellulose sources are the biomasses of plants, animals, bacteria, and algae.<sup>133</sup> Nowadays, plants (wood, cotton, vegetable fibers) are the most common cellulose sources.<sup>134</sup> Besides this, cellulose can be extracellularly produced by some bacteria. Currently, bacterial cellulose attracts significant attention because it is initially free of attendant bioproducts such as hemicelluloses, lignin, and pectin.<sup>135</sup> In addition to the above, industrial residues or municipal solid wastes (*e.g.* waste cotton clothes and cardboard) are currently considered as new environmentally friendly cellulose sources.<sup>136</sup>

The term “nanocellulose” implies cellulose in the form of structures that do not exceed 100 nm in size at least in one dimension, while in the other dimensions these structures can reach up to a few micrometres.<sup>6</sup> Compared to conventional cellulose, NC exhibits enhanced relative surface area along with tuneable mechanical, physical and chemical properties, which makes it a promising material for a wide range of applications including biomedical ones. Generally, depending on the origin and processing conditions three main types of NC can be distinguished: cellulose nanocrystals (CNCs), nanofibers (NFs), and bacterial cellulose (BC) (Fig. 7).

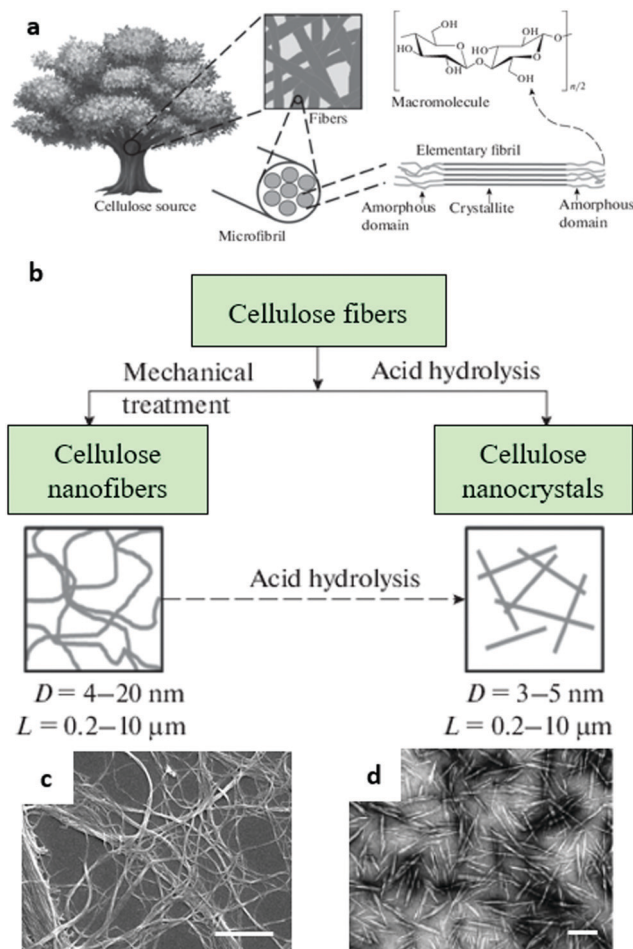


Fig. 7 (a) Hierarchical structure of cellulose and (b) synthesis of cellulose nanofibers and cellulose nanocrystals; adopted from ref. 143, copyright© 2018, Springer Nature. (c and d) SEM images of cellulose NFs and CNCs, respectively. (c) Adopted from ref. 144, copyright© 2013, Springer Nature. (d) Adopted from ref. 145, copyright© 2008, Royal Society of Chemistry.

CNCs have a rod-like structure with diameters of 5–60 nm and lengths of 100–500 nm. Typically, they are prepared by acid hydrolysis of cellulose, resulting in the destruction of amorphous regions, whereas the crystalline regions remain intact.<sup>137</sup> In turn, NFs have thicknesses up to 100 nm (or even more) and lengths up to several micrometres. These structures are generally prepared by enzymatic hydrolysis or high-pressure homogenization of cellulose,<sup>138</sup> although oxidative acid treatment may also be employed.<sup>139</sup> BC is also synthesized enzymatically from some bacteria.<sup>140</sup> It does not require additional purification steps as it initially possesses a higher purity along with a better crystallinity, degree of polymerization, and mechanical stability compared to other types of NC.

While HNTs and VCC have not yet been approved by the FDA for medical use, cellulosic materials are already widely used in medicine. Mostly, cellulose or its chemical derivatives are approved as materials for surgery devices (*e.g.* nonabsorbable gauze for internal use, §878.4450; nonresorbable gauze/sponge for external application, §878.4014); another example is cellulose-based contact lens intended to correct vision conditions (§886.5916). Besides this,



diluted suspensions of carboxymethylcellulose (CMC), hydroxyethylcellulose (HMC) and methylcelluloses are approved as ophthalmic demulcents under §349.12. Methylcellulose and CMC are substances generally recognised as safe (§582.1480 and §582.1745). A number of cellulose derivatives (ethyl-, hydroxypropyl-, methyl-ethyl-cellulose) are approved as direct additives to food for human consumption for multipurpose use (§172-I). In regard to this, the various types of NC seem to be promising for drug delivery and sustainable release.

#### 4.2. NC for drug delivery

**4.2.1. Drug loading and release.** The most common forms of drug carriers based on NC materials include nanoparticles, hydrogels, gels, membranes, and films. Nanoparticles are presented by drug loaded CNCs. CNCs are attractive due to their shape, biocompatibility, mechanical properties and ease of surface functionalization or bioconjugation. Intrinsically, CNCs have a large surface area and a negative surface charge, making them suitable for direct binding of hydrophilic drugs to their surfaces.<sup>141</sup> Similarly, NFs can also be loaded with small drugs.<sup>142</sup> Notably, adsorption of hydrophilic drugs with a high loading efficiency and enormous loading capacities can be achieved (e.g. up to 80% w/w for doxorubicin<sup>141</sup>). Furthermore, various surface modifications can be carried out on the hydroxyl groups to improve the affinity of CNCs to drugs that would not normally exhibit good binding, e.g. hydrophobic or uncharged drugs. Various chemical modification approaches are reviewed elsewhere.<sup>146,147</sup> For, instance, CNCs modified with chitosan can host about 14% w/w procaine hydrochloride (hydrophobic anesthetic drug).<sup>148</sup> CNCs modified with  $\beta$ -cyclodextrin were employed for delivery of curcumin that was harboured inside the cyclodextrin hydrophobic cavity with loading ratios 8 to 10% with respect to CNC mass.<sup>149</sup> Additionally, CNCs may be decorated with metal nanoparticles for preparation of composite structures, e.g. CNC/Ag and CNC/ZnO, have been proposed as effective antimicrobial agents,<sup>150</sup> whereas CNC/Au nanoparticles were used for further immobilization of enzymes.<sup>151</sup>

Besides direct use of NC as an excipient, it is often employed as a co-stabilizer to improve the physical-chemical properties of a polymeric matrix that can form beads. Usually, NC has a positive impact on the mechanical properties and the size distribution of the beads and therefore provides a better ability to pack the excipient, e.g. for tablet production. In such formulations, NC plays the role of a passive filler.<sup>152</sup>

One more biomedical application of CNCs is the preparation of gel-like structures, in particular hydro- and aero-gels. Overall, hydrogels are three-dimensional structures formed of linked polymer chains that are able to absorb and retain water without being dissolved. In fact, NC-based hydrogels differ from most other gels as their constructive elements are insoluble in water. This results in a different mechanism of gel network formation, which includes entanglement of NC particles or fibers followed by physical or chemical crosslinking.<sup>153</sup>

However, CNCs themselves lack the entanglement ability and more often are employed as fillers in gel composite structures due to their mechanical properties. In these composite hydrogels,

the interaction of CNCs with loaded molecules (drugs) usually does not affect the loading and release characteristics but significantly improves the mechanical and chemical stability of the hydrogels. Shojaeiarani *et al.* suggested the general classification of CNC containing hydrogels into two main groups with respect to their forms; the groups are bulk and injectable hydrogels.<sup>154</sup> The bulk hydrogels are prepared by free-radical polymerization of monomeric units with crosslinking agents to form three-dimensional structures. In turn, injectable hydrogels appear as polymer solutions with the ability to gel after injection, for instance, under physiological conditions. Moreover, they can go through reverse sol-gel transition triggered by external stimuli such as pH, temperature, electromagnetic fields, and UV-light. This makes injectable hydrogels promising candidates for drug delivery applications, as they are able to form a depot for sustainable drug release after injection with the possibility of remotely triggering a rapid drug release. While the use of nanoparticulate NC has relatively rarely been reported, NC-based hydrogels in the form of films, membranes and injectable gels have become increasingly popular for drug delivery applications, tissue regeneration and wound healing purposes.

Regardless of the form, the release from nano- and micro-particulate NC is mostly governed by diffusional transport that is often influenced by swelling in the case of the hydrogels.<sup>147,155</sup> Depending on chemical modification, the type of NC used (CNCs, NFs or BC), the form of formulation, and the microenvironment, the release can last from tens of minutes to a few months.<sup>147</sup> For instance, Li *et al.* prepared hybrid CNCs functionalised with folate and pH responsive multilayers that did not release the payload at pH 7.4 but released 95% of doxorubicin in 24 h at pH 5.5.<sup>156</sup> Integration of drugs into film-like matrix systems composed of NFs ensures their storage for almost three months at acidic pH for itraconazole and beclomethasone dipropionate in water.<sup>157</sup> More examples can be found in review 147.

**4.2.2. Cellular uptake, cytotoxicity and *in vivo* evaluation.** The cellular uptake and cytotoxicity of CNCs were studied with respect to both unmodified and functionalised NC materials. Dong *et al.* studied the cytotoxicity of CNCs with nine different cell lines and revealed no cytotoxic effects against any of the cell lines within the concentration range.<sup>158</sup> Similarly to HNTs, nonphagocytic cells take up rod-like CNCs mainly through non-specific endocytosis.<sup>158</sup> Later, the same group demonstrated specific cellular uptake through receptor-mediated endocytosis of CNCs conjugated with folic acid for folate receptor-positive cancer cells and destruction of cancer cells with internalized CNCs by irreversible electroporation.<sup>159</sup> Organic coatings of CNCs can have an effect on carrier cytotoxicity.<sup>160</sup> CNCs modified with polymers of various natures in comparison with bare CNCs on J774A.1 and MCF-7 cell lines have been tested. The results indicated that cells exposed to surface coated CNCs for 24 h did not show major changes in cell viability, membrane permeability, and cell morphology. However, the authors pointed that the longer periods of cell exposure require more careful examination. Mahmoud *et al.* demonstrated the ability of fluorescently labelled CNCs to penetrate the cell membrane without losing the membrane integrity and cytotoxicity effect.<sup>161</sup>



Interestingly, the cellular uptake was driven by the particle surface charge and the positively charged CNCs were easily internalized by cells unlike the negatively charged nanocrystals. The overall toxicity of the CNCs to the human organism with respect to the administration route and the overall dose still have to be investigated carefully as emphasized elsewhere.<sup>162</sup> Indeed, some reports indicate that use of NC leads to some long-term effects, e.g. NFs non-specifically decrease the intestinal absorption *in vivo*.<sup>163</sup> It is worth mentioning that the low toxicity of NC-based materials does not guarantee the safety of chemically modified NC. Therefore, careful evaluation of NC-derivatives should be performed in case of every modification. For instance, recently the hepatotoxicity of NC modified with oxalate ester has been reported.<sup>164</sup>

The performance of injectable and bulk CNC hybrid hydrogels was widely investigated *in vitro* and *in vivo*. As some recent *in vivo* examples, de France *et al.* studied tissue response and biodistribution of CNC/poly(oligoethyleneglycol methacrylate) injectable hydrogels.<sup>165</sup> They found that the hydrogel is mainly localized in the injection site and its components did not accumulate in any organ. Additionally, the hydrogel induced moderate inflammatory response and promoted fibroblast proliferation *in vivo*. Magnetic bulk hydrogel beads for pH-triggered release of anticancer drug dexamethasone in the gastro-intestinal tract have been reported.<sup>166</sup> Karzar Jeddi and Mahkam noted that inclusion of 2% (wt) of CNCs improved the swelling degree, drug loading capacity, and drug release behavior of the hydrogel composites. pH sensitive composite dialdehyde CNC/chitosan hydrogels loaded with theophylline were tested *in vitro*.<sup>167</sup>

### 4.3. NC for tissue engineering

Cellulose-based hydrogels are extremely attractive for tissue engineering. In recent years, various methods have been proposed for the processing of hydrogels based on NC. The architecture of NC can be engineered from the nano- to macro-scale that, together with excellent biocompatibility and mechanical properties, allows producing scaffolds particularly suitable for use in tissue regeneration. Generally, NC-based scaffolds are composites wherein NC is employed in combination with other polymers or particles. The role of NC is usually in providing the required mechanical stability and chemical resistance to hydrolytic and enzymatic degradation.

Thus, Ghavimi *et al.* employed CNCs to prepare CNC/chitosan hydrogels with mechanical properties mimicking vertebral bones to treat vertebral compression fractures.<sup>168</sup> Silva *et al.* prepared a composite hyaluronic acid/CNC/tropoelastin hydrogel as a cell growing substrate.<sup>169</sup> The incorporation of CNCs improved the hydrogel's stability against hydrolytic and enzymatic degradation due to the chemical bonding of CNCs and hyaluronic acid. The resulting gels were shown to support and promote cell adhesion, viability and growth, which is indispensable for tissue engineering and regeneration applications. Alternatively, for cell growth applications Kumar *et al.* prepared polysaccharide hydrogels reinforced with halloysites and CNCs.<sup>170</sup> The mechanical properties of these hydrogels can be controlled by variation of CNCs and halloysite amount in the gel composition.

The applications of NC-based composite hydrogels in tissue engineering are highly versatile and may cover bone tissue engineering, cornea treatment, heart and vascular muscle regeneration and many other relevant applications as reviewed elsewhere.<sup>171</sup>

Currently, the development of advanced wound dressing materials is probably one of the most attractive areas of NC-based materials. The advanced healing strategies imply non-invasive monitoring of tissue recovery, pain management and controlled release of drugs accelerating regeneration and minimizing scar formation.<sup>172</sup>

In regard to this, currently hydrogels prepared with various forms of NC are intensively studied including those which are sensitive to various external stimuli. Xu *et al.* employed CNCs to improve the mechanical properties of thermo-responsive chitosan/glycerol phosphate sodium injectable hydrogels.<sup>173</sup> The resulting hydrogels were loaded with human umbilical cord-mesenchymal stem cells that are able to produce cytokines and growth factors promoting wound healing. The gels were tested for cutaneous wound healing in experiments *in vivo* and demonstrated accelerated wound closure and skin regeneration. Huang *et al.* described an injectable hydrogel prepared using carboxymethylchitosan and dialdehyde modified CNCs.<sup>174</sup> The gel demonstrated very good biocompatibility, self-healing and on-demand solubilisation under mildly acidic conditions. The gel was tested as a wound-healing agent in a deep partial thickness skin burn model *in vivo* and was shown to be effective for burn surface covering and treatment. Du *et al.* reported gel microparticles prepared *via* Schiff-base reaction between carboxymethylchitosan and oxidized CMC and loaded with BSA or silver sulfadiazine demonstrating alkaline and acid responsive drug release and antibacterial properties against *S. aureus* and *E. coli* bacteria when silver sulfadiazine was used.<sup>175</sup> In turn, Yan *et al.* prepared a pH-responsive hydrogel combining CMC, HCM and dopamine. The resulting hydrogel demonstrated a bacteriostatic effect that was maintained for five days.<sup>176</sup>

Another way for the preparation of a pH-responsive hydrogel *via* radical polymerization was proposed by Park *et al.*<sup>177</sup> The resulting hydrogel was loaded with flavonoid naringenin to prepare a transdermal delivery system for treatment of atopic skin conditions disbalancing skin pH. The hydrogel effectively wetted the skin, improving drug penetration. An interesting approach for preparation of antimicrobial wound dressing cellulose hydrogels was proposed by Shen *et al.*<sup>178</sup> They employed mesoporous silica nanoparticles SBA-15 coated with CaCO<sub>3</sub> to prevent their degradation during the preparation of an SBA-15/cellulose composite. The sustainable antibacterial activity against *S. aureus* and *E. coli* was figured out to be 144 h at its longest.

As NC hydrogels may act as both wound dressing materials (Fig. 8) and scaffolds for cell culture, Loh *et al.* employed bacterial NC/acrylic acid hydrogels to heal wounds requiring exogenous cells for tissue regeneration.<sup>179</sup> To do this, human epidermal keratinocytes and dermal fibroblasts were enclosed into a gel matrix. The cells were mostly attached to the hydrogel within 4 h. In turn, the gel was shown to provide cell viability and free transfer to the wound site. The wound healing ability



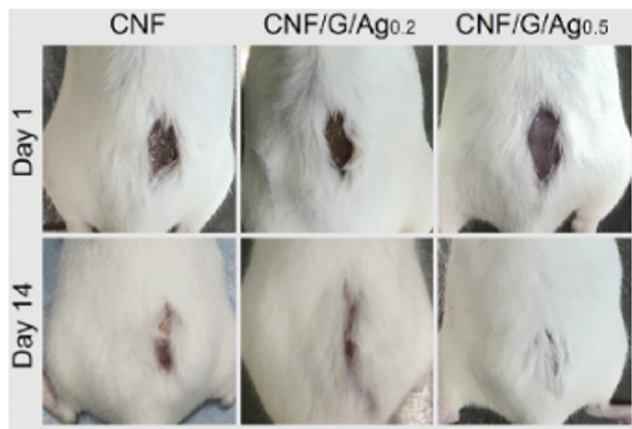


Fig. 8 Photographs of mice treated with different wound dressing scaffolds: carboxylated cellulose nanofibers (CNFs) and two composite CNF–gelatine scaffolds (CNF/G/Ag) functionalised with silver nanoparticles (0.2 and 0.5 wt%, respectively). Adopted from ref. 180, copyright© 2018 Elsevier.

of the cell-loaded hydrogel was estimated in experiments *in vivo* in a full-thickness wound model. The wound was almost completely closed (about 99%) in two weeks of gel treatment.

Additionally, Pöttinger *et al.* employed BC as a gene activated matrix for prolonged release of loaded plasmids for site-specific gene delivery.<sup>181</sup> Plasmids can be efficiently immobilized in a cellulose matrix providing their prolonged release up to 50 days. The depot for sustainable and targeted delivery of plasmids may be promising for wound healing of soft tissues due to the delivery of plasmids encoding for growth factors of platelets, fibroblasts or brain derived neurotrophic factors.<sup>182</sup> The formation of hard tissues like cartilage or bones can be promoted as well by delivering the genes encoding for bone morphogenetic proteins, which control bone differentiation and ossification.<sup>183</sup> In addition, wound dressing materials loaded with plasmids encoding for vascular endothelial growth factors or angiogenin triggering the formation of new blood vessels may accelerate angiogenesis.<sup>184</sup>

## 5. Summary and prospects

For the convenience of the reader, the key physical–chemical properties that determine the characteristics of vehicles considered for drug delivery and tissue engineering are summarized in Table 2. Each of these three vehicles can be found in nature or synthesized from natural sources using simple and low-cost technologies. In the age when the rapid and effective establishment of large-scale production, which at the same time should necessarily be ecologically friendly, is one of the main requirements for successful translation from science to industry, it is not surprising that research on naturally derived HNTs, VCC and NC is actively developing. Being animal- and plant-free materials that can be found literally beneath your feet or isolated from wastes, HNTs, VCC and NC have high potential to revolutionise drug vehicle production. On the other hand, green and sustainable production is the only thing that unites these vehicles, since each of them exhibits unique properties.

Table 2 Summary of the physical–chemical properties of halloysite nanotubes, vaterite crystals and cellulose nanocrystals

Vehicle Shape	Dimensions	ζ-Potential at		S <sub>(BET)</sub> , m <sup>2</sup> g <sup>-1</sup>	Pore Ø, nm	Density, g cm <sup>-3</sup>	Young's modulus, GPa	Surface groups for chemical modification
		pH 7, mV	Internal Ø					
HNTs	Hollow tubes Length 0.5–2 µm, outer Ø 20–200 nm	–(13–40) <sup>17</sup> –(185–187)	Internal Ø 10–70 nm <sup>3,1,186</sup>	30–65 <sup>186,188</sup>	10–60 nm <sup>81,191</sup>	2.55–2.65 (Mineralogy Database)	10–460, average 140 <sup>189</sup>	Lumen surface: Al–OH groups, suitable for chemical grafting (e.g. organosilanes) External surface: Si–OH groups, chemically inert, suitable for physical adsorption of cationic surfactants and polymers <sup>190</sup> Surfaces are not suitable for chemical modification but can be used for physical adsorption, e.g. for polymer multilayer deposition <sup>102</sup> Multiple –OH groups suitable for various modifications <i>via</i> oxidation, esterification, fluorescent labelling, click chemistry, etc. <sup>196</sup>
VCC	Porous spheres Ø 50 nm–70 µm	+(11–15) <sup>82</sup>	10–60 nm <sup>81,191</sup>	3–20 <sup>70,191</sup>	10–60 nm <sup>81,191</sup>	2.54 (Mineralogy Database)	60–86 <sup>192</sup>	
CNCs	Rods Length 100–200 nm, Ø 3–5 nm	–(70–100) <sup>187,193</sup>	Non-porous	400–500 <sup>194</sup>	Non-porous	~1.5–1.6 <sup>195</sup>	100–130 <sup>195</sup>	

<sup>a</sup> Negative charge on the external surface and positive charge on the internal surface over a broad pH range.



Their diverse shapes, sizes, surface charges, and mechanical properties as well as different mechanisms of entrapment and release of molecules give the opportunity to choose the most suitable vehicle depending on the specific biomedical task. This gives the vehicles equal chances for future development and bioapplications and opens broad and new avenues for their utilisation in biomedicine.

Although the studies of HNTs, VCC and NC toward biomedical applications have significantly advanced in recent years, now it is too premature to speak about the introduction of HNTs, VCC and NC into biomedicine. This is because this research is still relatively new that perhaps has not even fully reached the stage of clinical trials. While low levels of cytotoxicity were verified for HNTs, VCC and NC on various cell lines and bioassays, the number of *in vivo* studies is still very limited. Some other questions also remain unanswered. For instance, the mechanisms of cellular responses to HNTs, VCC and NC should be better described and understood. This especially concerns VCC which potentially may cause a misbalance in Ca<sup>2+</sup> metabolism. Internalization mechanisms for delivery into a cell also should be investigated. These studies should be consistent with the design of new vehicles based on functionalised HNTs, VCC and NC that may can expand the range of their application, enhance cellular uptake and improve drug delivery.

In the next years, we expect the surge of *in vitro* and *in vivo* evaluation of the performance of HNTs, VCC and NC as delivery vehicles. Further this research might be smoothly translated to clinical trials that will be a huge step in the development of these naturally derived delivery vehicles.

The fact that kaolin clays, calcium carbonate and cellulose are approved by the FDA for food supplementation and medical uses might significantly simplify the approval of HNTs, VCC and NC for drug delivery purposes. This gives an enormous advantage to HNTs, VCC and NC in contrast to many other delivery vehicles.

Together with the low production costs and availability of the vehicles considered here, they may swiftly find their niche in drug delivery with high potential to outpace their analogues.

Finally, tissue engineering and repair applications of HNTs, VCC and NC deserve specific attention but other fields are expected for future applications.

Herein, HNTs do not form the core of the scaffold but can be used as an additive for scaffold functionalisation. Cosmetic applications of HNTs would be expected due to their low toxicity and ability to host and release materials in a sustained and controlled way.

VCC is an important example for bone tissue engineering; its future applications are expected in intracellular delivery due to its complete degradation as well as in dentistry due to its use as a source of calcium ions that is now achieved mostly using amorphous CaCO<sub>3</sub> that has no defined structure. Applications of VCC in cosmetics would also be desirable because of its highly controlled release and ability to encapsulate virtually any molecules.

NC that can serve as the core material for a scaffold for various tissues particularly stands out. At the same time,

NC-based scaffolds seem to be promising for orthopaedic and other surgical applications due to their high biocompatibility and an option to make films and membranes with desired characteristics. However, more studies on controlled fabrication and functionalisation are expected in the nearest future.

In addition to the above, new technologies for up-scalable controlled bottom-up production of VCC and NC and new methods for HNT purification/modification and NC isolation from wastes are upcoming. Finally, the combination of these natural materials will be one of the future trends that would allow merging their properties and therefore building a better platform for tissue growth. Scaffolds with unique active properties demonstrating a dynamic crosstalk with a regenerating tissue are expected as a result of hybrid materials made using combinations of HNTs, VCC and NC. These materials belong to the third generation of biomaterials where the dynamics of bio-signals of extracellular matrices is recapitulated within advanced active scaffolds.

## Conflicts of interest

There are no conflicts to declare.

## Acknowledgements

A. V. acknowledges the European Union's Horizon 2020 research and innovation programme (Marie-Curie Individual Fellowship LIGHTOPLEX-747245). This work was supported by a Russian Scientific Fund, Grant no. 19-79-30091.

## References

- H. He, Q. Liang, M. C. Shin, K. Lee, J. Gong, J. Ye, Q. Liu, J. Wang and V. Yang, *Front. Chem. Sci. Eng.*, 2013, 7, 496–507.
- Y. Zhang, H. F. Chan and K. W. Leong, *Adv. Drug Delivery Rev.*, 2013, 65, 104–120.
- R. Kanwar, J. Rathee, D. B. Salunke and S. K. Mehta, *ACS Omega*, 2019, 4, 8804–8815.
- H. Jahangirian, E. G. Lemraski, T. J. Webster, R. Rafiee-Moghaddam and Y. Abdollahi, *Int. J. Nanomed.*, 2017, 12, 2957–2978.
- E. J. Cho, L. T. P. Trinh, Y. Song, Y. G. Lee and H.-J. Bae, *Bioresour. Technol.*, 2020, 298, 122386.
- L. Bacakova, J. Pajorova, M. Bacakova, A. Skogberg, P. Kallio, K. Kolarova and V. Svorcik, *Nanomaterials*, 2019, 9, e164.
- M. C. Barros, P. M. Bello, M. Bao and J. J. Torrado, *J. Cleaner Prod.*, 2009, 17, 400–407.
- D. Cree and A. Rutter, *ACS Sustainable Chem. Eng.*, 2015, 3, 941–949.
- G. Cavallaro, G. Lazzara and R. Fakhrullin, *Ther. Delivery*, 2018, 9, 287–301.
- R. M. Hazen, D. A. Sverjensky, D. Azzolini, D. L. Bish, S. C. Elmore, L. Hinnov and R. E. Milliken, *Am. Mineral.*, 2013, 98, 2007–2029.



- 11 M. Liu, R. Fakhrullin, A. Novikov, A. Panchal and Y. Lvov, *Macromol. Biosci.*, 2019, **19**, e1800419.
- 12 Y. M. Lvov, D. G. Shchukin, H. Möhwald and R. R. Price, *ACS Nano*, 2008, **2**, 814–820.
- 13 J. Keeling, in *Natural Mineral Nanotubes*, ed. P. Pasbakhsh and G. Churchman, Apple Academic Press, 2015, vol. 32, pp. 95–116.
- 14 Y. Lvov and E. Abdullayev, *Prog. Polym. Sci.*, 2013, **38**, 1690–1719.
- 15 Y. M. Lvov, M. M. DeVilliers and R. F. Fakhrullin, *Expert Opin. Drug Delivery*, 2016, **13**, 977–986.
- 16 S. Satish, M. Tharmavaram and D. Rawtani, *Nanobiomedicine*, 2019, **6**, DOI: 10.1177/1849543519863625.
- 17 Y. Yang, Y. Chen, F. Leng, L. Huang, Z. Wang and W. Tian, *Appl. Sci.*, 2017, **7**, 1215.
- 18 D. Tan, P. Yuan, F. Annabi-Bergaya, D. Liu, L. Wang, H. Liu and H. He, *Appl. Clay Sci.*, 2014, **96**, 50–55.
- 19 M. Massaro, G. Lazzara, S. Milioto, R. Noto and S. Riela, *J. Mater. Chem. B*, 2017, **5**, 2867–2882.
- 20 A. M. Yamina, M. Fizir, A. Itatahine, H. He and P. Dramou, *Colloids Surf., B*, 2018, **170**, 322–329.
- 21 H. Li, X. Zhu, J. Xu, W. Peng, S. Zhong and Y. Wang, *RSC Adv.*, 2016, **6**, 54463–54470.
- 22 R. Yendluri, Y. Lvov, M. M. de Villiers, V. Vinokurov, E. Naumenko, E. Tarasova and R. Fakhrullin, *J. Pharm. Sci.*, 2017, **106**, 3131–3139.
- 23 Y. Hu, J. Chen, X. Li, Y. Sun, S. Huang, Y. Li, H. Liu, J. Xu and S. Zhong, *Nanotechnology*, 2017, **28**, 375101.
- 24 A. Stavitskaya, S. Batasheva, V. Vinokurov, G. Fakhrullina, V. Sangarov, Y. Lvov and R. Fakhrullin, *Nanomaterials*, 2019, **9**, E708.
- 25 (a) Y.-F. Shi, Z. Tian, Y. Zhang, H.-B. Shen and N.-Q. Jia, *Nanoscale Res. Lett.*, 2011, **6**, 608; (b) Z. Long, J. Zhang, Y. Shen, C. Zhou and M. Liu, *Mater. Sci. Eng., C*, 2017, **81**, 224–235.
- 26 V. Khodzhaeva, A. Makeeva, V. Ulyanova, P. Zelenikhin, V. Evtugyn, M. Hardt, E. Rozhina, Y. Lvov, R. Fakhrullin and O. Ilinskaya, *Front. Pharmacol.*, 2017, **8**, 631.
- 27 A. V. Stavitskaya, A. A. Novikov, M. S. Kotelev, D. S. Kopitsyn, E. V. Rozhina, I. R. Ishmukhametov, R. F. Fakhrullin, E. V. Ivanov, Y. M. Lvov and V. A. Vinokurov, *Nanomaterials*, 2018, **8**, E391.
- 28 (a) S. A. Konnova, Y. M. Lvov and R. F. Fakhrullin, *Clay Miner.*, 2016, **51**, 429–433; (b) Y. Lvov, A. Panchal, Y. Fu, R. Fakhrullin, M. Kryuchkova, S. Batasheva, A. Stavitskaya, A. Glotov and V. Vinokurov, *Langmuir*, 2019, **35**, 8646–8657.
- 29 V. A. Vinokurov, A. V. Stavitskaya, A. P. Glotov, A. A. Novikov, A. V. Zolotukhina, M. S. Kotelev, P. A. Gushchin, E. V. Ivanov, Y. Darrat and Y. M. Lvov, *Chem. Rec.*, 2018, **18**, 858–867.
- 30 G. Lazzara, G. Cavallaro, A. Panchal, R. Fakhrullin, A. Stavitskaya, V. Vinokurov and Y. Lvov, *Curr. Opin. Colloid Interface Sci.*, 2018, **35**, 42–50.
- 31 M. Fizir, P. Dramou, N. S. Dahiru, W. Ruya, T. Huang and H. He, *Microchim. Acta*, 2018, **185**, 389.
- 32 R. Yendluri, D. P. Otto, M. M. de Villiers, V. Vinokurov and Y. M. Lvov, *Int. J. Pharm.*, 2017, **521**, 267–273.
- 33 F. R. Ahmed, M. H. Shoaib, R. I. Yousuf, T. Ali, K. E. Geckeler, F. Siddiqui, K. Ahmed and F. Qazi, *Eur. J. Pharm. Sci.*, 2019, **133**, 214–227.
- 34 L. Lisuzzo, G. Cavallaro, S. Milioto and G. Lazzara, *New J. Chem.*, 2019, **43**, 10887–10893.
- 35 H. Lun, J. Ouyang and H. Yang, *RSC Adv.*, 2014, **4**, 44197–44202.
- 36 E. G. Bediako, E. Nyankson, D. Dodoo-Arhin, B. Agyei-Tuffour, D. Łukowiec, B. Tomiczek, A. Yaya and J. K. Efavi, *Heliyon*, 2018, **4**, e00689.
- 37 G. Cavallaro, G. Lazzara, M. Massaro, S. Milioto, R. Noto, F. Parisi and S. Riela, *J. Phys. Chem. C*, 2015, **119**, 8944–8951.
- 38 P. Dramou, M. Fizir, A. Taleb, A. Itatahine, N. S. Dahiru, Y. A. Mehdi, L. Wei, J. Zhang and H. He, *Carbohydr. Polym.*, 2018, **197**, 117–127.
- 39 M. R. Dзамukova, E. A. Naumenko, Y. M. Lvov and R. F. Fakhrullin, *Sci. Rep.*, 2015, **5**, 10560.
- 40 A. C. Santos, C. Ferreira, F. Veiga, A. J. Ribeiro, A. Panchal, Y. Lvov and A. Agarwal, *Adv. Colloid Interface Sci.*, 2018, **257**, 58–70.
- 41 M. Massaro, R. Amorati, G. Cavallaro, S. Guernelli, G. Lazzara, S. Milioto, R. Noto, P. Poma and S. Riela, *Colloids Surf., B*, 2016, **140**, 505–513.
- 42 H. Liu, Z.-G. Wang, S.-L. Liu, X. Yao, Y. Chen, S. Shen, Y. Wu and W. Tian, *J. Mater. Sci.*, 2019, **54**, 693–704.
- 43 E. Rozhina, A. Panchal, F. Akhatova, Y. Lvov and R. Fakhrullin, *Appl. Clay Sci.*, 2019, 105371.
- 44 (a) S. A. Konnova, I. R. Sharipova, T. A. Demina, Y. N. Osin, D. R. Yarullina, O. N. Ilinskaya, Y. M. Lvov and R. F. Fakhrullin, *Chem. Commun.*, 2013, **49**, 4208–4210; (b) V. Vergaro, E. Abdullayev, Y. M. Lvov, A. Zeitoun, R. Cingolani, R. Rinaldi and S. Leporatti, *Biomacromolecules*, 2010, **11**, 820–826.
- 45 X. Lai, M. Agarwal, Y. M. Lvov, C. Pachpande, K. Varahramyan and F. A. Witzmann, *J. Appl. Toxicol.*, 2013, **33**, 1316–1329.
- 46 G. I. Fakhrullina, F. S. Akhatova, Y. M. Lvov and R. F. Fakhrullin, *Environ. Sci.: Nano*, 2015, **2**, 54–59.
- 47 Z. Long, Y.-P. Wu, H.-Y. Gao, J. Zhang, X. Ou, R.-R. He and M. Liu, *J. Mater. Chem. B*, 2018, **6**, 7204–7216.
- 48 R. F. Kamaliev, I. R. Ishmukhametov, S. N. Batasheva, E. V. Rozhina and R. F. Fakhrullin, *Nano-Struct. Nano-Objects*, 2018, **15**, 54–60.
- 49 J. Liao, S. Peng, M. Long, Y. Zhang, H. Yang, Y. Zhang and J. Huang, *Colloids Surf., A*, 2020, **586**, 124242.
- 50 (a) X. Wang, J. Gong, Z. Gui, T. Hu and X. Xu, *Environ. Toxicol.*, 2018, **33**, 623–630; (b) X. Wang, J. Gong, R. Rong, Z. Gui, T. Hu and X. Xu, *J. Agric. Food Chem.*, 2018, **66**, 2925–2933.
- 51 G. Y. Kırımlioğlu, Y. Yazan, K. Erol and Ç. Çengelli Ünel, *Int. J. Pharm.*, 2015, **495**, 816–826.
- 52 N. Kerdsakundee, W. Li, J. P. Martins, Z. Liu, F. Zhang, M. Kemell, A. Correia, Y. Ding, M. Airavaara, J. Hirvonen, R. Wiwattanapatapee and H. A. Santos, *Adv. Healthcare Mater.*, 2017, **6**, 1700629.
- 53 A. Panchal, G. Fakhrullina, R. Fakhrullin and Y. Lvov, *Nanoscale*, 2018, **10**, 18205–18216.
- 54 G. Fakhrullina, E. Khakimova, F. Akhatova, G. Lazzara, F. Parisi and R. Fakhrullin, *ACS Appl. Mater. Interfaces*, 2019, **11**, 23050–23064.



- 55 L. Yang, Y.-C. Lee, M. I. Kim, H. G. Park, Y. S. Huh, Y. Shao and H.-K. Han, *J. Mater. Chem. B*, 2014, **2**, 7567–7574.
- 56 R. Rong, Y. Zhang, Y. Zhang, Y. Hu, W. Yang, X. Hu, L. Wen and Q. Zhang, *Nanotoxicology*, 2019, **13**, 354–368.
- 57 (a) *Functional Polymer Composites with Nanoclays*, ed. Y. Lvov, B. Guo and R. F. Fakhruddin, Royal Society of Chemistry, Cambridge, UK, 2017, vol. 22; (b) E. Naumenko and R. Fakhruddin, *Biotechnol. J.*, 2019, **14**, e1900055.
- 58 T. S. Gaaz, A. B. Sulong, M. N. Akhtar, A. A. H. Kadhum, A. B. Mohamad and A. A. Al-Amiery, *Molecules*, 2015, **20**, 22833–22847.
- 59 S. S. Suner, S. Demirci, B. Yetiskin, R. Fakhruddin, E. Naumenko, O. Okay, R. S. Ayyala and N. Sahiner, *Int. J. Biol. Macromol.*, 2019, **130**, 627–635.
- 60 E. A. Naumenko, I. D. Guryanov, R. Yendluri, Y. M. Lvov and R. F. Fakhruddin, *Nanoscale*, 2016, **8**, 7257–7271.
- 61 X. Zhang, R. Guo, J. Xu, Y. Lan, Y. Jiao, C. Zhou and Y. Zhao, *J. Biomater. Appl.*, 2015, **30**, 512–525.
- 62 W. Wei, E. Abdullayev, A. Hollister, D. Mills and Y. M. Lvov, *Macromol. Mater. Eng.*, 2012, **297**, 645–653.
- 63 O. S. Manoukian, M. R. Arul, S. Rudraiah, I. Kalajzic and S. G. Kumbar, *J. Controlled Release*, 2019, **296**, 54–67.
- 64 G. Sandri, C. Aguzzi, S. Rossi, M. C. Bonferoni, G. Bruni, C. Boselli, A. I. Cornaglia, F. Riva, C. Viseras, C. Caramella and F. Ferrari, *Acta Biomater.*, 2017, **57**, 216–224.
- 65 Y. Zhang, K. Huang, Q. Yuan, Z. Gu and G. Wu, *J. Biomed. Nanotechnol.*, 2019, **15**, 1909–1922.
- 66 M. Chozhanathmisra, D. Govindaraj, P. Karthikeyan, K. Pandian, L. Mitu and R. Rajavel, *J. Chem.*, 2018, **2018**, 1–12.
- 67 A. G. Christy, *Cryst. Growth Des.*, 2017, **17**, 3567–3578.
- 68 C. Rodriguez-Navarro, C. Jimenez-Lopez, A. Rodriguez-Navarro, M. T. Gonzalez-Muñoz and M. Rodriguez-Gallego, *Geochim. Cosmochim. Acta*, 2007, **71**, 1197–1213.
- 69 P. Bots, L. G. Benning, J.-D. Rodriguez-Blanco, T. Roncal-Herrero and S. Shaw, *Cryst. Growth Des.*, 2012, **12**, 3806–3814.
- 70 N. Feoktistova, J. Rose, V. Z. Prokopović, A. S. Vikulina, A. Skirtach and D. Volodkin, *Langmuir*, 2016, **32**, 4229–4238.
- 71 D. Gebauer, A. Völkel and H. Cölfen, *Science*, 2008, **322**, 1819–1822.
- 72 Z. Dong, L. Feng, W. Zhu, X. Sun, M. Gao, H. Zhao, Y. Chao and Z. Liu, *Biomaterials*, 2016, **110**, 60–70.
- 73 D. B. Trushina, T. V. Bukreeva and M. N. Antipina, *Cryst. Growth Des.*, 2016, **16**, 1311–1319.
- 74 D. B. Trushina, S. N. Sulyanov, T. V. Bukreeva and M. V. Kovalchuk, *Crystallogr. Rep.*, 2015, **60**, 570–577.
- 75 L.-f. Yang, D.-q. Chu, H.-l. Sun and G. Ge, *New J. Chem.*, 2016, **40**, 571–577.
- 76 A. Sergeeva, R. Sergeev, E. Lengert, A. Zakharevich, B. Parakhonskiy, D. Gorin, S. Sergeev and D. Volodkin, *ACS Appl. Mater. Interfaces*, 2015, **7**, 21315–21325.
- 77 P. V. Binevski, N. G. Balabushevich, V. I. Uvarova, A. S. Vikulina and D. Volodkin, *Colloids Surf., B*, 2019, **181**, 437–449.
- 78 S. Maleki Dizaj, M. Barzegar-Jalali, M. H. Zarrintan, K. Adibkia and F. Lotfipour, *Expert Opin. Drug Delivery*, 2015, **12**, 1649–1660.
- 79 D. B. Trushina, T. N. Borodina, S. N. Sulyanov, J. V. Moiseeva, N. V. Gulyaeva and T. V. Bukreeva, *Crystallogr. Rep.*, 2018, **63**, 998–1004.
- 80 (a) S. Maleki Dizaj, F. Lotfipour, M. Barzegar-Jalali, M.-H. Zarrintan and K. Adibkia, *Artif. Cells, Nanomed., Biotechnol.*, 2017, **45**, 535–543; (b) M. Y. Memar, K. Adibkia, S. Farajnia, H. S. Kafil, S. Maleki Dizaj and R. Ghotaslou, *J. Drug Delivery Sci. Technol.*, 2019, **54**, 101307.
- 81 A. S. Vikulina, N. A. Feoktistova, N. G. Balabushevich, A. G. Skirtach and D. Volodkin, *Phys. Chem. Chem. Phys.*, 2018, **20**, 8822–8831.
- 82 N. A. Feoktistova, A. S. Vikulina, N. G. Balabushevich, A. G. Skirtach and D. Volodkin, *Mater. Des.*, 2020, **185**, 108223.
- 83 D. W. Green, B. J. R. F. Bolland, J. M. Kanczler, S. A. Lanham, D. Walsh, S. Mann and R. O. C. Oreffo, *Biomaterials*, 2009, **30**, 1918–1927.
- 84 P. Zhao, S. Wu, Y. Cheng, J. You, Y. Chen, M. Li, C. He, X. Zhang, T. Yang, Y. Lu, R. J. Lee, X. He and G. Xiang, *Nanomedicine*, 2017, **13**, 2507–2516.
- 85 C.-Q. Wang, J.-L. Wu, R.-X. Zhuo and S.-X. Cheng, *Mol. Biosyst.*, 2014, **10**, 672–678.
- 86 M. Długosz, M. Bulwan, G. Kania, M. Nowakowska and S. Zapotoczny, *J. Nanopart. Res.*, 2012, **14**, 1313.
- 87 T. V. Bukreeva, I. V. Marchenko, T. N. Borodina, I. V. Degtev, S. L. Sitnikov, Y. V. Moiseeva, N. V. Gulyaeva and M. V. Kovalchuk, *Dokl. Phys. Chem.*, 2011, **440**, 165–167.
- 88 R. F. Fakhruddin, A. G. Bikmullin and D. K. Nurgaliev, *ACS Appl. Mater. Interfaces*, 2009, **1**, 1847–1851.
- 89 J. R. Lakkakula, R. Kurapati, I. Tynga, H. Abrahamse, A. M. Raichur and R. W. Macedo Krause, *RSC Adv.*, 2016, **6**, 104537–104548.
- 90 V. E. Bosio, M. L. Cacicedo, B. Calvignac, I. León, T. Beuvier, F. Boury and G. R. Castro, *Colloids Surf., B*, 2014, **123**, 158–169.
- 91 N. G. Balabushevich, E. A. Kovalenko, I. M. Le-Deygen, L. Y. Filatova, D. Volodkin and A. S. Vikulina, *Mater. Des.*, 2019, **182**, 108020.
- 92 N. G. Balabushevich, A. V. Lopez de Guereñu, N. A. Feoktistova, A. G. Skirtach and D. Volodkin, *Macromol. Biosci.*, 2016, **16**, 95–105.
- 93 S. V. German, M. V. Novoselova, D. N. Bratashov, P. A. Demina, V. S. Atkin, D. V. Voronin, B. N. Khlebtsov, B. V. Parakhonskiy, G. B. Sukhorukov and D. A. Gorin, *Sci. Rep.*, 2018, **8**, 17763.
- 94 N. G. Balabushevich, A. V. Lopez de Guereñu, N. A. Feoktistova and D. Volodkin, *Phys. Chem. Chem. Phys.*, 2015, **17**, 2523–2530.
- 95 J. Song, R. Wang, Z. Liu and H. Zhang, *Mol. Med. Rep.*, 2018, **17**, 8403–8408.
- 96 A. S. Sergeeva, E. K. Volkova, D. N. Bratashov, M. I. Shishkin, V. S. Atkin, A. V. Markin, A. A. Skaptsov, D. V. Volodkin and D. A. Gorin, *Thin Solid Films*, 2015, **583**, 60–69.
- 97 D. B. Trushina, R. A. Akasov, A. V. Khovankina, T. N. Borodina, T. V. Bukreeva and E. A. Markvicheva, *J. Mol. Liq.*, 2019, **284**, 215–224.
- 98 C. Correa-Paz, M. F. Navarro Poupard, E. Polo, M. Rodríguez-Pérez, P. Taboada, R. Iglesias-Rey, P. Hervella, T. Sobrino,



- D. Vivien, J. Castillo, P. Del Pino, F. Campos and B. Pelaz, *J. Controlled Release*, 2019, **308**, 162–171.
- 99 N. G. Balabushevich, E. A. Sholina, E. V. Mikhalechik, L. Y. Filatova, A. S. Vikulina and D. Volodkin, *Micromachines*, 2018, **9**, E307.
- 100 N. Feoktistova, G. Stoychev, N. Pureskiy, L. Ionov and D. Volodkin, *Eur. Polym. J.*, 2015, **68**, 650–656.
- 101 (a) D. V. Volodkin, A. I. Petrov, M. Prevot and G. B. Sukhorukov, *Langmuir*, 2004, **20**, 3398–3406; (b) L. L. del Mercato, P. Rivera-Gil, A. Z. Abbasi, M. Ochs, C. Ganas, I. Zins, C. Sönnichsen and W. J. Parak, *Nanoscale*, 2010, **2**, 458–467; (c) A. S. Timin, D. J. Gould and G. B. Sukhorukov, *Expert Opin. Drug Delivery*, 2017, **14**, 583–587; (d) M. S. Saveleva, K. Eftekhari, A. Abalymov, T. E. L. Douglas, D. Volodkin, B. V. Parakhonskiy and A. G. Skirtach, *Front. Chem.*, 2019, **7**, 179; (e) S. Zhao, F. Caruso, L. Dähne, G. Decher, B. G. de Geest, J. Fan, N. Feliu, Y. Gogotsi, P. T. Hammond, M. C. Hersam, A. Khademhosseini, N. Kotov, S. Leporatti, Y. Li, F. Lisdat, L. M. Liz-Marzán, S. Moya, P. Mulvaney, A. L. Rogach, S. Roy, D. G. Shchukin, A. G. Skirtach, M. M. Stevens, G. B. Sukhorukov, P. S. Weiss, Z. Yue, D. Zhu and W. J. Parak, *ACS Nano*, 2019, **13**, 6151–6169; (f) A. S. Vikulina, A. G. Skirtach and D. Volodkin, *Langmuir*, 2019, **35**, 8565–8573.
- 102 D. Volodkin, *Colloid Polym. Sci.*, 2014, **292**, 1249–1259.
- 103 A. Wang, Y. Yang, X. Zhang, X. Liu, W. Cui and J. Li, *ChemPlusChem*, 2016, **81**, 194–201.
- 104 A. Som, R. Raliya, L. Tian, W. Akers, J. E. Ippolito, S. Singamaneni, P. Biswas and S. Achilefu, *Nanoscale*, 2016, **8**, 12639–12647.
- 105 H. Li, Y. Zhao, Y. Jia, C. Qu and J. Li, *Chem. Commun.*, 2019, **55**, 15057–15060.
- 106 (a) B. V. Parakhonskiy, A. M. Yashchenok, S. Donatan, D. V. Volodkin, F. Tessarolo, R. Antolini, H. Möhwald and A. G. Skirtach, *ChemPhysChem*, 2014, **15**, 2817–2822; (b) A. Hernández-Hernández, A. B. Rodríguez-Navarro, J. Gómez-Morales, C. Jiménez-Lopez, Y. Nys and J. M. García-Ruiz, *Cryst. Growth Des.*, 2008, **8**, 1495–1502.
- 107 H. M. Burt, J. K. Jackson, D. R. Taylor and R. S. Crowther, *Dig. Dis. Sci.*, 1997, **42**, 1283–1289.
- 108 B. V. Parakhonskiy, C. Foss, E. Carletti, M. Fedel, A. Haase, A. Motta, C. Migliaresi and R. Antolini, *Biomater. Sci.*, 2013, **1**, 1273.
- 109 Y. I. Svenskaya, A. M. Pavlov, D. A. Gorin, D. J. Gould, B. V. Parakhonskiy and G. B. Sukhorukov, *Colloids Surf., B*, 2016, **146**, 171–179.
- 110 S. A. Kamba, M. Ismail, S. H. Hussein-Al-Ali, T. A. T. Ibrahim and Z. A. B. Zakaria, *Molecules*, 2013, **18**, 10580–10598.
- 111 S. Donatan, A. Yashchenok, N. Khan, B. Parakhonskiy, M. Cocquyt, B.-E. Pinchasik, D. Khalkenow, H. Möhwald, M. Konrad and A. Skirtach, *ACS Appl. Mater. Interfaces*, 2016, **8**, 14284–14292.
- 112 H. Cao, Y. Yang, Y. Qi, Y. Li, B. Sun, Y. Li, W. Cui, J. Li and J. Li, *Adv. Healthcare Mater.*, 2018, **7**, e1701357.
- 113 G. Choukrani, B. Maharjan, C. H. Park, C. S. Kim and A. R. Kurup Sasikala, *Mater. Sci. Eng., C*, 2020, **106**, 110226.
- 114 J. Chen, X. Wang, Y. Liu, H. Liu, F. Gao, C. Lan, B. Yang, S. Zhang and Y. Gao, *Chem. Eng. J.*, 2019, **369**, 394–402.
- 115 (a) T. N. Borodina, D. B. Trushina, I. V. Marchenko and T. V. Bukreeva, *J. Bionanosci.*, 2016, **6**, 261–268; (b) N. G. Balabushevich, E. A. Kovalenko, E. V. Mikhalechik, L. Y. Filatova, D. Volodkin and A. S. Vikulina, *J. Colloid Interface Sci.*, 2019, **545**, 330–339.
- 116 Y. I. Svenskaya, E. A. Genina, B. V. Parakhonskiy, E. V. Lengert, E. E. Talnikova, G. S. Terentyuk, S. R. Utz, D. A. Gorin, V. V. Tuchin and G. B. Sukhorukov, *ACS Appl. Mater. Interfaces*, 2019, **11**, 17270–17282.
- 117 O. Gusliakova, E. N. Atochina-Vasserman, O. Sindeeva, S. Sindeev, S. Pinyaev, N. Pyataev, V. Revin, G. B. Sukhorukov, D. Gorin and A. J. Gow, *Front. Pharmacol.*, 2018, **9**, 559.
- 118 M. S. Saveleva, A. A. Abalymov, G. P. Lyubun, I. V. Vidyasheva, A. M. Yashchenok, T. E. L. Douglas, D. A. Gorin and B. V. Parakhonskiy, *J. Biomed. Mater. Res., Part A*, 2017, **105**, 94–103.
- 119 A. Sergeeva, N. Feoktistova, V. Prokopovic, D. Gorin and D. Volodkin, *Adv. Mater. Interfaces*, 2015, **2**, 1500386.
- 120 R. Schröder, H. Pohlitz, T. Schüler, M. Panthöfer, R. E. Unger, H. Frey and W. Tremel, *J. Mater. Chem. B*, 2015, **3**, 7079–7089.
- 121 Y. Gong, Y. Zhang, Z. Cao, F. Ye, Z. Lin and Y. Li, *Biomater. Sci.*, 2019, **7**, 3614–3626.
- 122 M. S. Saveleva, A. N. Ivanov, M. O. Kurtukova, V. S. Atkin, A. G. Ivanova, G. P. Lyubun, A. V. Martyukova, E. I. Cherevko, A. K. Sargsyan, A. S. Fedonnikov, I. A. Norkin, A. G. Skirtach, D. A. Gorin and B. V. Parakhonskiy, *Mater. Sci. Eng., C*, 2018, **85**, 57–67.
- 123 A. Obata, H. Ozasa, T. Kasuga and J. R. Jones, *J. Mater. Sci.: Mater. Med.*, 2013, **24**, 1649–1658.
- 124 Y. S. Liu, Q. L. Huang, A. Kienzle, W. E. G. Müller and Q. L. Feng, *Mater. Sci. Eng., C*, 2014, **38**, 227–234.
- 125 (a) A. Obata, T. Hotta, T. Wakita, Y. Ota and T. Kasuga, *Acta Biomater.*, 2010, **6**, 1248–1257; (b) T. Kasuga, A. Obata, H. Maeda, Y. Ota, X. Yao and K. Oribe, *J. Mater. Sci.: Mater. Med.*, 2012, **23**, 2349–2357; (c) K. Fujikura, S. Lin, J. Nakamura, A. Obata and T. Kasuga, *J. Biomed. Mater. Res., Part B*, 2013, **101**, 1350–1358.
- 126 A. Stoica-Guzun, M. Stroescu, S. I. Jinga, I. M. Jipa and T. Dobre, *Ind. Crops Prod.*, 2013, **50**, 414–422.
- 127 S. Yamazaki, H. Maeda, A. Obata, K. Inukai, K. Kato and T. Kasuga, *J. Nanomater.*, 2012, **2012**, 1–7.
- 128 A. S. Sergeeva, D. A. Gorin and D. V. Volodkin, *Langmuir*, 2015, **31**, 10813–10821.
- 129 T. Paulraj, N. Feoktistova, N. Velk, K. Uhlig, C. Duschl and D. Volodkin, *Macromol. Rapid Commun.*, 2014, **35**, 1408–1413.
- 130 A. Sergeeva, A. S. Vikulina and D. Volodkin, *Micromachines*, 2019, **10**, 357.
- 131 (a) B. Lindman, G. Karlström and L. Stigsson, *J. Mol. Liq.*, 2010, **156**, 76–81; (b) B. Medronho and B. Lindman, *Adv. Colloid Interface Sci.*, 2015, **222**, 502–508.
- 132 F. A. Ngwabebhoh and U. Yildiz, *J. Appl. Polym. Sci.*, 2019, **136**, 47878.
- 133 S. Gopi, P. Balakrishnan, D. Chandradhara, D. Poovathankandy and S. Thomas, *Mater. Today Chem.*, 2019, **13**, 59–78.





- 134 E. Pinho and G. Soares, *J. Mater. Chem. B*, 2018, **6**, 1887–1898.
- 135 C. Sharma and N. K. Bhardwaj, *Mater. Sci. Eng., C*, 2019, **104**, 109963.
- 136 Y. W. Chen and H. V. Lee, *Int. J. Biol. Macromol.*, 2018, **107**, 78–92.
- 137 A. Karimian, H. Parsian, M. Majidinia, M. Rahimi, S. M. Mir, H. S. Kafil, V. Shafiei-Irannejad, M. Kheyrollah, H. Ostadi and B. Yousefi, *Int. J. Biol. Macromol.*, 2019, **133**, 850–859.
- 138 S. Salimi, R. Sotudeh-Gharebagh, R. Zarghami, S. Y. Chan and K. H. Yuen, *ACS Sustainable Chem. Eng.*, 2019, **7**, 15800–15827.
- 139 A. A. Novikov, B. M. Anikushin, D. A. Petrova, S. A. Konstantinova, V. B. Mel'nikov and V. A. Vinokurov, *Chem. Technol. Fuels Oils*, 2018, **54**, 564–568.
- 140 H. Ullah, H. A. Santos and T. Khan, *Cellulose*, 2016, **23**(2), 291–2314.
- 141 J. K. Jackson, K. Letchford, B. Z. Wasserman, L. Ye, W. Y. Hamad and H. M. Burt, *Int. J. Nanomed.*, 2011, **6**, 321–330.
- 142 G. Sarkar, J. T. Orasugh, N. R. Saha, I. Roy, A. Bhattacharyya, A. K. Chattopadhyay, D. Rana and D. Chattopadhyay, *New J. Chem.*, 2017, **41**, 15312–15319.
- 143 A. O. Malakhov, T. S. Anokhina, D. A. Petrova, V. A. Vinokurov and A. V. Volkov, *Pet. Chem.*, 2018, **58**, 923–933.
- 144 S. Varanasi, R. He and W. Batchelor, *Cellulose*, 2013, **20**(1), 885–1896.
- 145 Y. Habibi, A.-L. Goffin, N. Schiltz, E. Duquesne, P. Dubois and A. Dufresne, *J. Mater. Chem.*, 2008, **18**, 5002.
- 146 J. B. Daud and K.-Y. Lee, in *Handbook of Nanocellulose and Cellulose Nanocomposites*, ed. H. Kargarzadeh, I. Ahmad, S. Thomas and A. Dufresne, Wiley-VCH Verlag GmbH & Co. KGaA, Weinheim, Germany, 2017, vol. 280, pp. 101–122.
- 147 N. Lin and A. Dufresne, *Eur. Polym. J.*, 2014, **59**, 302–325.
- 148 S. P. Akhlaghi, R. C. Berry and K. C. Tam, *Cellulose*, 2013, **20**, 1747–1764.
- 149 G. M. A. Ndong Ntoutoume, R. Granet, J. P. Mbakidi, F. Brégier, D. Y. Léger, C. Fidanzi-Dugas, V. Lequart, N. Joly, B. Liagre, V. Chaleix and V. Sol, *Bioorg. Med. Chem. Lett.*, 2016, **26**, 941–945.
- 150 (a) S. Azizi, M. Ahmad, M. Mahdavi and S. Abdolmohammadi, *BioResources*, 2013, **8**, 1841–1851; (b) H. Liu, J. Song, S. Shang, Z. Song and D. Wang, *ACS Appl. Mater. Interfaces*, 2012, **4**, 2413–2419.
- 151 K. A. Mahmoud, K. B. Male, S. Hrapovic and J. H. T. Luong, *ACS Appl. Mater. Interfaces*, 2009, **1**, 1383–1386.
- 152 (a) R. Kolakovic, L. Peltonen, T. Laaksonen, K. Putkisto, A. Laukkanen and J. Hirvonen, *AAPS PharmSciTech*, 2011, **12**, 1366–1373; (b) J. C. O. Villanova, E. Ayres, S. M. Carvalho, P. S. Patrício, F. V. Pereira and R. L. Oréfice, *Eur. J. Pharm. Sci.*, 2011, **42**, 406–415.
- 153 R. Curvello, V. S. Raghuvanshi and G. Garnier, *Adv. Colloid Interface Sci.*, 2019, **267**, 47–61.
- 154 J. Shojaeiarani, D. Bajwa and A. Shirzadifar, *Carbohydr. Polym.*, 2019, **216**, 247–259.
- 155 L. Pachuau, in *Nanocellulose and Nanohydrogel Matrices*, ed. M. Jawaid and F. Mohammad, Wiley-VCH Verlag GmbH & Co. KGaA, Weinheim, Germany, 2017, vol. 2, pp. 1–19.
- 156 N. Li, H. Zhang, Y. Xiao, Y. Huang, M. Xu, D. You, W. Lu and J. Yu, *Biomacromolecules*, 2019, **20**, 937–948.
- 157 R. Kolakovic, L. Peltonen, A. Laukkanen, J. Hirvonen and T. Laaksonen, *Eur. J. Pharm. Biopharm.*, 2012, **82**, 308–315.
- 158 S. Dong, A. A. Hirani, K. R. Colacino, Y. W. Lee and M. Roman, *Nano LIFE*, 2012, **02**, 1241006.
- 159 S. Dong, H. J. Cho, Y. W. Lee and M. Roman, *Biomacromolecules*, 2014, **15**, 1560–1567.
- 160 A. S. Jimenez, F. Jaramillo, U. D. Hemraz, Y. Boluk, K. Ckless and R. Sunasee, *Nanotechnol., Sci. Appl.*, 2017, **10**, 123–136.
- 161 K. A. Mahmoud, J. A. Mena, K. B. Male, S. Hrapovic, A. Kamen and J. H. T. Luong, *ACS Appl. Mater. Interfaces*, 2010, **2**, 2924–2932.
- 162 (a) M. Roman, *Ind. Biotechnol.*, 2015, **11**, 25–33; (b) A. B. Seabra, J. S. Bernardes, W. J. Favaro, A. J. Paula and N. Duran, *Carbohydr. Polym.*, 2018, **181**, 514–527.
- 163 Y. Chen, Y.-J. Lin, T. Nagy, F. Kong and T. L. Guo, *Carbohydr. Polym.*, 2020, **229**, 115536.
- 164 C. A. Otuechere, A. Adewuyi, O. L. Adebayo and I. A. Ebigwei, *Hum. Exp. Toxicol.*, 2020, **39**, 212–223.
- 165 K. J. de France, M. Badv, J. Dorogin, E. Siebers, V. Panchal, M. Babi, J. Moran-Mirabal, M. Lawlor, E. D. Cranston and T. Hoare, *ACS Biomater. Sci. Eng.*, 2019, **5**, 2235–2246.
- 166 M. Karzar Jeddi and M. Mahkam, *Int. J. Biol. Macromol.*, 2019, **135**, 829–838.
- 167 Q. Xu, Y. Ji, Q. Sun, Y. Fu, Y. Xu and L. Jin, *Nanomaterials*, 2019, **9**, E253.
- 168 S. A. A. Ghavimi, E. S. Lungren, T. J. Faulkner, M. A. Josselet, Y. Wu, Y. Sun, F. M. Pfeiffer, C. L. Goldstein, C. Wan and B. D. Ulery, *Int. J. Biol. Macromol.*, 2019, **130**, 88–98.
- 169 C. R. Silva, P. S. Babo, S. Mithieux, R. M. Domingues, R. Reis, M. E. Gomes and A. Weiss, *J. Biomater. Appl.*, 2019, **34**, 560–572.
- 170 A. Kumar, I. A. I. Matari, H. Choi, A. Kim, Y. J. Suk, J. Y. Kim and S. S. Han, *Mater. Sci. Eng., C*, 2019, **104**, 109983.
- 171 (a) S. van Vlierberghe, P. Dubruel and E. Schacht, *Biomacromolecules*, 2011, **12**, 1387–1408; (b) S. D. Dutta, D. K. Patel and K.-T. Lim, *J. Biol. Eng.*, 2019, **13**, 55.
- 172 A. Gupta, M. Kowalczyk, W. Heaselgrave, S. T. Britland, C. Martin and I. Radecka, *Eur. Polym. J.*, 2019, **111**, 134–151.
- 173 H. Xu, S. Huang, J. Wang, Y. Lan, L. Feng, M. Zhu, Y. Xiao, B. Cheng, W. Xue and R. Guo, *Int. J. Biol. Macromol.*, 2019, **137**, 433–441.
- 174 W. Huang, Y. Wang, Z. Huang, X. Wang, L. Chen, Y. Zhang and L. Zhang, *ACS Appl. Mater. Interfaces*, 2018, **10**, 41076–41088.
- 175 S. Du, X. Chen, X. Chen, S. Li, G. Yuan, T. Zhou, J. Li, Y. Jia, D. Xiong and H. Tan, *Macromol. Chem. Phys.*, 2019, **220**, 1900399.
- 176 Q. Yan, L. Liu, T. Wang and H. Wang, *Colloid Polym. Sci.*, 2019, **297**, 705–717.
- 177 S. H. Park, H. S. Shin and S. N. Park, *Carbohydr. Polym.*, 2018, **200**, 341–352.
- 178 Z. Shen, N. Cai, Y. Xue, V. Chan, B. Yu, J. Wang, H. Song, H. Deng and F. Yu, *Polymers*, 2019, **11**, E808.



- 179 E. Y. X. Loh, N. Mohamad, M. B. Fauzi, M. H. Ng, S. F. Ng and M. C. I. Mohd Amin, *Sci. Rep.*, 2018, **8**, 2875.
- 180 R. Liu, L. Dai, C. Si and Z. Zeng, *Carbohydr. Polym.*, 2018, **195**, 63–70.
- 181 Y. Poetzinger, L. Rahnfeld, D. Kralisch and D. Fischer, *Carbohydr. Polym.*, 2019, **209**, 62–73.
- 182 H. Storrie and D. J. Mooney, *Adv. Drug Delivery Rev.*, 2006, **58**, 500–514.
- 183 S. D'Mello, K. Atluri, S. M. Geary, L. Hong, S. Elangovan and A. K. Salem, *AAPS J.*, 2017, **19**, 43–53.
- 184 Y. Mo, R. Guo, Y. Zhang, W. Xue, B. Cheng and Y. Zhang, *Tissue Eng., Part A*, 2017, **23**, 597–608.
- 185 Q. Pan, N. Li, Y. Hong, H. Tang, Z. Zheng, S. Weng, Y. Zheng and L. Huang, *RSC Adv.*, 2017, **7**, 21352–21359.
- 186 Y. Joo, J. H. Sim, Y. Jeon, S. U. Lee and D. Sohn, *Chem. Commun.*, 2013, **49**, 4519–4521.
- 187 V. Vinokurov, A. Novikov, V. Rodnova, B. Anikushin, M. Kotelev, E. Ivanov and Y. Lvov, *Polymers*, 2019, **11**, E919.
- 188 C. Li, Y. Zhao, T. Zhu, Y. G. Li, J. Ruan and G. Li, *RSC Adv.*, 2018, **8**, 14870–14878.
- 189 B. Lecouvet, J. Horion, C. D'Haese, C. Bailly and B. Nysten, *Nanotechnology*, 2013, **24**, 105704.
- 190 D. Tan, P. Yuan, D. Liu and P. Du, *Nanosized Tubular Clay Minerals – Halloysite and Imogolite*, Elsevier, 2016, vol. 7, pp. 167–201.
- 191 D. B. Trushina, T. V. Bukreeva, M. V. Kovalchuk and M. N. Antipina, *Mater. Sci. Eng., C*, 2014, **45**, 644–658.
- 192 (a) R. Ševčík, P. Šašek and A. Viani, *J. Mater. Sci.*, 2018, **53**, 4022–4033; (b) X. Feng and S. A. T. Redfern, *Geochim. Cosmochim. Acta*, 2018, **236**, 351–360.
- 193 Z. Hosseinidou, M. N. Alam, G. Sim, N. Tufenkji and T. G. M. van de Ven, *Nanoscale*, 2015, **7**, 16647–16657.
- 194 A. Brinkmann, M. Chen, M. Couillard, Z. J. Jakubek, T. Leng and L. J. Johnston, *Langmuir*, 2016, **32**, 6105–6114.
- 195 A. Dufresne, *Mater. Today*, 2013, **16**, 220–227.
- 196 S. Eyley and W. Thielemans, *Nanoscale*, 2014, **6**, 7764–7779.

